(2)

NUSC Technical Document 8229
29 February 1988

Electromagnetic Interference (EMI) Performance of Shield Ground Adapters and Composite Materials

Presentations Made at the 1987 IEEE International Symposium on Electromagnetic Compatibility

David S. Dixon
Submarine Electromagnetic Systems Department

James V. Masi
Western New England College

Naval Underwater Systems Center
Newport, Rhode Island / New London, Connecticut

Preface

This document was prepared under Project No. A51000, The Ships Below-Decks Electromagnetic Compatibility (EMC) Program, Principal Investigator D.S. Dixon (Code 3431). The Sponsoring Activity is the Office of The Chief of Naval Research/ Office of Naval Technology; Submarine Technology Program Element Manager, G. Remmers (Code 233). The Submarine Technology Block Program Manager is L. Cathers (Code 012.4) of the David W. Taylor Naval Ship Research and Development Center.

Important contributions required to conduct the work were made by G & H Technology, Inc., and Western New England College under contract to the Naval Underwater Systems Center (NUSC).

The authors wish to acknowledge the contribution of John Miller, EMC consultant for G & H Technology, Inc., who provided the triaxial fixture test method measurement data for the shield ground adapters.

Reviewed and Approved:

D. F. Dence

D.F. Dence
Submarine Electromagnetic Systems Department

UNCLASSIFIED
SECURITY CLASSIFICATION OF THIS PAGE

REPORT DOCUMENTATION PAGE

1a. REPORT SECURITY CLASSIFICATION UNCLASSIFIED	1b. RESTRICTIVE MARKINGS
2a. SECURITY CLASSIFICATION AUTHORITY	3. DISTRIBUTION/AVAILABILITY OF REPORT Approved for public release; distribution unlimited.
2b. DECLASSIFICATION/DOWNGRADING SCHEDULE	
4. PERFORMING ORGANIZATION REPORT NUMBER(S) TD8229	5. MONITORING ORGANIZATION REPORT NUMBER(S)
6a. NAME OF PERFORMING ORGANIZATION Naval Underwater Systems Center 6b. OFFICE SYMBOL (If applicable)	7a. NAME OF MONITORING ORGANIZATION
6c. ADDRESS (City, State, and ZIP Code) New London Laboratory New London, CT 06320-5594	7b. ADDRESS (City, State, and ZIP Code)
8a. NAME OF FUNDING/SPONSORING ORGANIZATION OCNR/ONT 8b. OFFICE SYMBOL (If applicable) Code 233	9. PROCUREMENT INSTRUMENT IDENTIFICATION NUMBER
8c. ADDRESS (City, State, and ZIP Code) Washington, DC 20362	10. SOURCE OF FUNDING NUMBERS PROGRAM ELEMENT NO. 62323N PROJECT NO. RB23C55 TASK NO. WORK UNIT ACCESSION NO.

11. TITLE (Include Security Classification)
Electromagnetic Interference (EMI) Performance of Shield Ground Adapters and Composite Materials

12. PERSONAL AUTHOR(S)
Dixon, David S. and Dr. James V. Masi

13a. TYPE OF REPORT	13b. TIME COVERED	14. DATE OF REPORT (Year, Month, Day)	15. PAGE COUNT
Technical	FROM 8-25-87 TO 8-27-87	1988 FEB 29	66

16. SUPPLEMENTARY NOTATION
Presentations Made at the 1987 IEEE International Symposium on Electromagnetic Compatibility

17. COSATI CODES			18. SUBJECT TERMS (Continue on reverse if necessary and identify by block number)
FIELD	GROUP	SUB-GROUP	
17	04		~~EMC~~ Composite Connectors, EMI ~~Crosstalk~~, EMI/EMP Protection, Shielding Performance of Materials, Shield Ground Adapters.
11	04		

19. ABSTRACT (Continue on reverse if necessary and identify by block number)

1. "Long Term EMI Performance of Several Shield Ground Adapters" (presented by David S. Dixon) proved that, if the degradation caused by the kickpipe threads can be reduced, a new technology shield ground adapter (SGA), with a solid shield contactor, will ensure the highest long term SGA performance, thereby reducing below-decks electromagnetic (EM) levels caused by EMI/ electromagnetic pulse (EMP) cable currents.

2. "Development of a Full Performance Composite Connector with Long Term EMI Shielding Properties" (presented by James V. Masi) discusses development of a full MIL-SPEC connector made from composite materials that was designed to satisfy a full range of EM, chemical, and mechanical properties. A mathematical model was developed to give a basis for predicting some of the EM properties of a composite material. Keywords.

20. DISTRIBUTION/AVAILABILITY OF ABSTRACT ☒ UNCLASSIFIED/UNLIMITED ☐ SAME AS RPT. ☐ DTIC USERS	21. ABSTRACT SECURITY CLASSIFICATION UNCLASSIFIED
22a. NAME OF RESPONSIBLE INDIVIDUAL David S. Dixon	22b. TELEPHONE (Include Area Code) (203) 440-4453 22c. OFFICE SYMBOL 3431

DD FORM 1473, 84 MAR — 83 APR edition may be used until exhausted. All other editions are obsolete.

SECURITY CLASSIFICATION OF THIS PAGE
UNCLASSIFIED

TABLE OF CONTENTS

PRESENTATION MATERIAL

PUBLISHED PAPERS

FOREWORD

This document contains presentation materials pertaining to the electromagnetic interference (EMI) performance of shield ground adapters (SGA's) and composite materials that were presented at the 1987 IEEE International Symposium on Electromagnetic Compatibility. Section 1 contains the materials for the presentation on the EMI performance of SGA's as well as a summary of the author's presentation remarks. The published paper related to this presentation is found in appendix A. Section 2 contains the materials for the presentation on the EMI performance of composite materials. The published paper related to this presentation is found in appendix B.

SECTION 1

LONG TERM PERFORMANCE OF SEVERAL SHIELD GROUND ADAPTERS (SGA's)

INTRODUCTION

LONG TERM PERFORMANCE OF SEVERAL SHIELD GROUND ADAPTERS (SGAs)

PRESENTED BY

DAVID S. DIXON

NAVAL UNDERWATER SYSTEMS CENTER

NEW LONDON, CT

Appreciation expressed to:

- Co-authors
  - Stan Sherman (formerly of NUSC).
  - Mike Van Brunt (G & H Technology).
- Mike Van Brunt and John Miller for providing post-installation SGA test data.

SHIELD GROUND ADAPTER (SGA) PRESENTATION ORGANIZATION

- *BACKGROUND/HISTORY*
- *TRANSFER IMPEDANCE MEASUREMENTS*
- *COMPARISON OF MEASURED/MODELED A.C. DATA*
- *SHIPBOARD INSTALLATION & D.C. TESTING*
- *SGA A.C. PERFORMANCE -VS- TIME*
- *IMPROVED SGA*
- *CONCLUSIONS*
- *RECOMMENDATIONS*

BACKGROUND

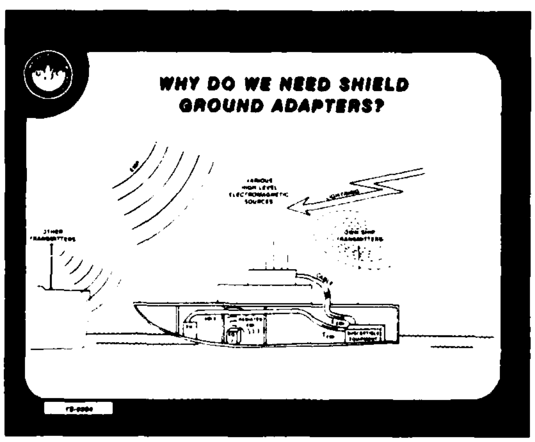

- High-level EM sources capable of significant coupling to electronic/electrical cables and systems:
  - Lightning.
  - Nearby transmitters.
  - Electromagnetic pulse (EMP).

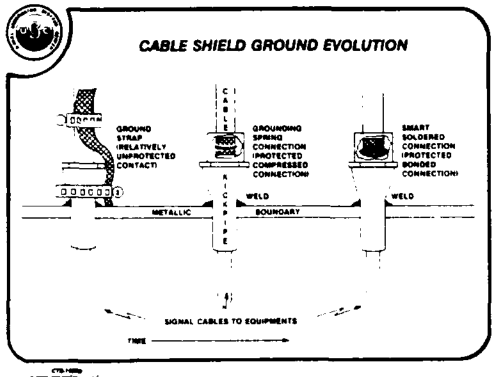

As illustrated:

- Cable shield ground evolution began with simple ground straps and hose clamps.
- Second Generation: Grounding ring or rings using an environmentally protected, compression type adapter.
- Improved Second Generation: Smart-soldered connection to cable shield and a protected adapter.

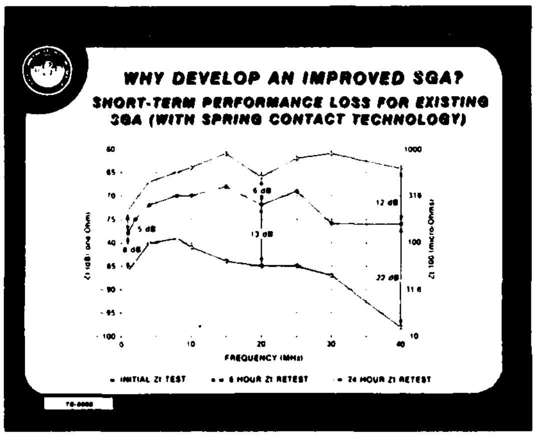

One of the major driving forces to develop a new SGA was the rapid change in the existing SGA's performance with time:

- Bottom Curve: Initial performance.
- Middle Curve: Performance degradation of 8 to 22 dB after 6 hours.
- Top Curve: Performance degradation ranging from 13 to 34 dB after 24 hours.

SGA PHYSICAL MODELS

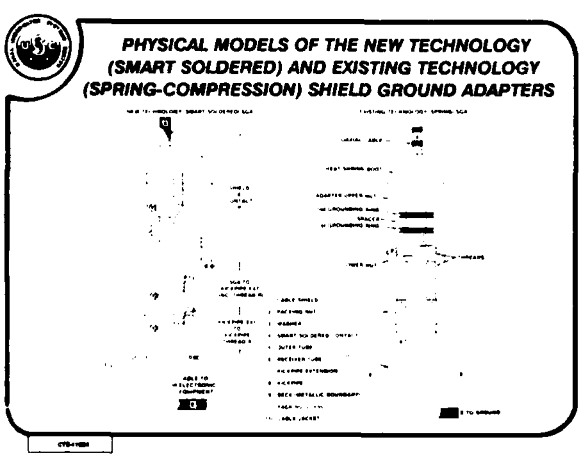

- Left: New Technology SGA.
- Right: Existing Technology SGA.
- New Technology SGA (left) dc test points:
  - A to B -- Cable shield plus shield contactor with SGA.
  - B to C -- First SGA thread interface.
  - C to D -- Second thread interface; exists only for the shipboard test case.
  - E to GRD -- Shield-to-ground voltage inside ship; measurement of SGA performance.

SHIELD CONTACTOR DESIGN

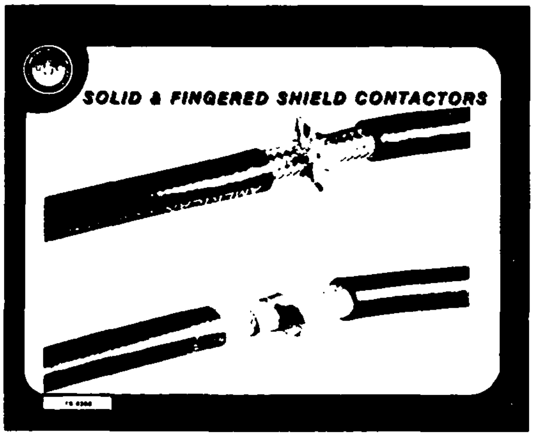

- Top: Original shield contactor design. Slotted/fingered design easy to manufacture.
- Bottom: Improved, almost solid shield contactor design that improved performance by up to 35 dB over the fingered design (top).
- One of the last viewgraphs will illustrate this improvement in performance.

SHIPBOARD INSTALLATION FOR REALISTIC LONG TERM ENVIRONMENTAL EXPOSURE

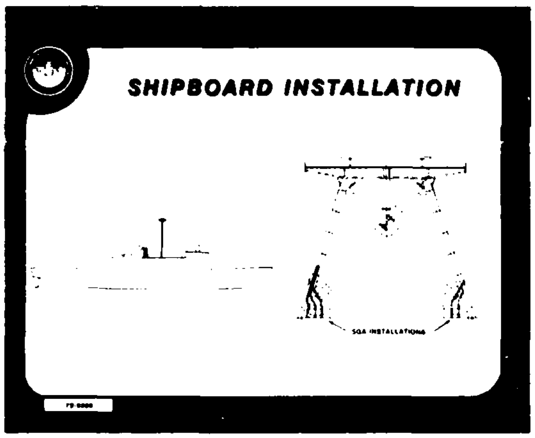

- Available platform and kickpipes.
- SGA's were mounted at base of two legs of the antenna platform.

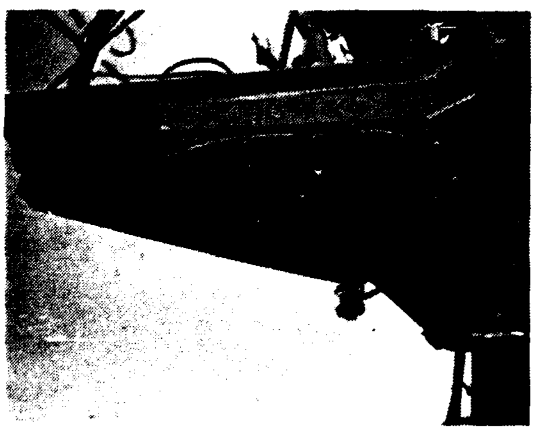

- Topside portion of the cable terminated in brass junction box.
- Realistic corrosion and cable currents due to nearby transmitters.

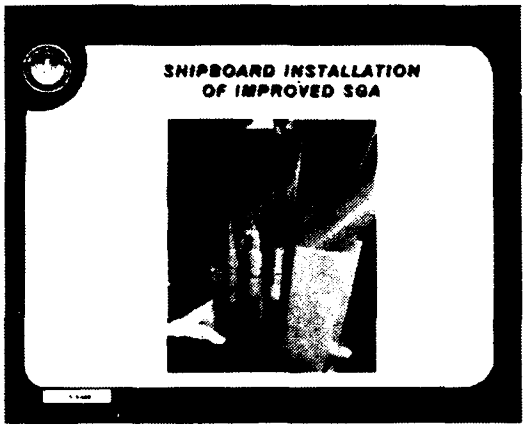

- Closeup view of two existing SGA's plus one of the two SGA's installed on the ship.
- Second SGA installed at base of the other platform leg.

MEASUREMENT PROCEDURES: DC ON SHIP; AC IN LAB (NUSC/G & H)

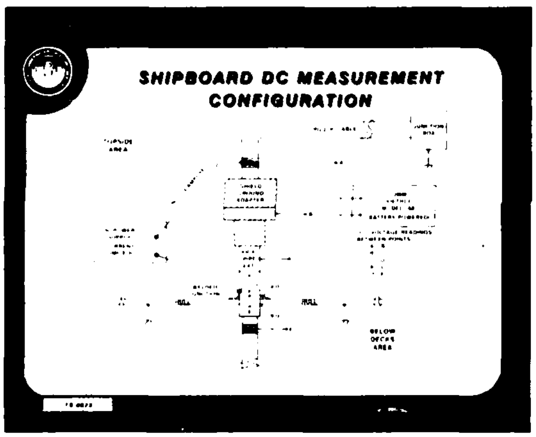

Ship measurement: DC only:

- I = 4 A on cable/through SGA.
- Measurements points A through E:
  - A to B: Cable shield and shield contactor.
  - B to C: First thread interface.
  - C to D: Second thread interface (ship test only).
  - E to GRD: SGA output voltage -- measure of SGA performance.

NUSC LABORATORY MEASUREMENTS

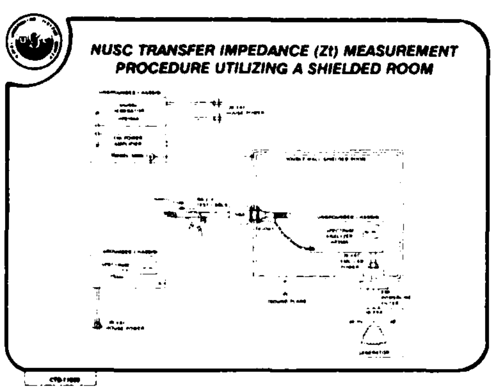

- Measurement technique good to approximately 30 MHz.
- I shield ≈ 4 A.
- V shield-to-ground terminated by spectrum analyzer 50 Ω input Z.
- Double-wall shielded room served as boundary between protected and unprotected spaces.

G & H TECHNOLOGY TEST FIXTURE

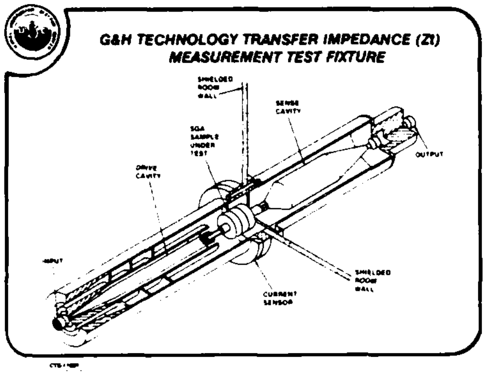

- Triaxial fixture operated in shorted coax mode.
- Performance good to at least 200 MHz.
- Also utilizes shielded room as boundary.
- Incorporates an Inconel current sensor built into fixture.

TEST DATA MEASUREMENTS

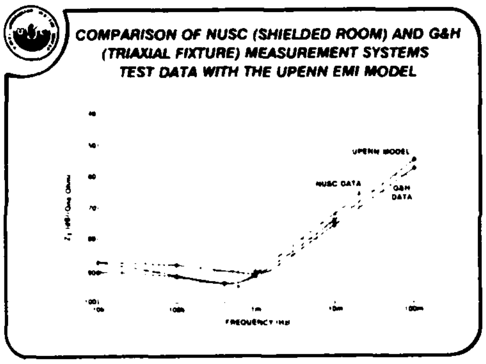

Due to variations in post-installation, test data measurements were conducted by NUSC and G & H on the same SGA and were compared with the UPenn SGA model.

- Within 4 dB of each other.
- Measurements taken approximately 1 week apart (East Coast/West Coast).
- Different fixtures and test equipment.

DC TRANSFER Z MEASUREMENTS
INITIAL MEASUREMENTS/6 MONTHS/12 MONTHS

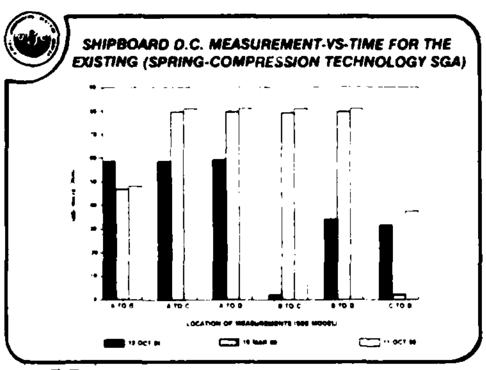

<u>Existing Technology SGA</u>:

- Initial dc performance dominated by A to B resistance.
- A to B: Improves slightly with time.
- B to C: First thread junction caused degradation.

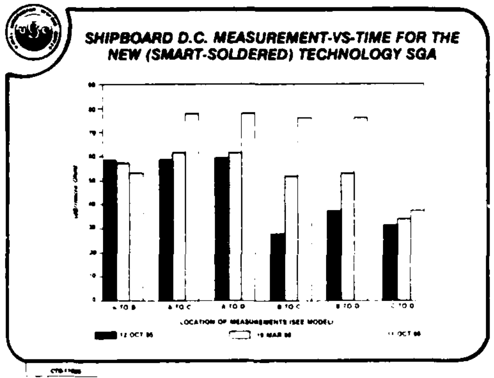

New Technology SGA -- As with existing technology SGA:

- A to B: Dominated initial SGA performance.
- A to B: Improved slightly with time.
- B to C: Threads took longer than 6 months to degrade.
- After degrading thread area dominated SGA performance.

AC TRANSFER Z MEASUREMENTS
NUSC -- PRE- AND POST-INSTALLATION; G & H -- POST-INSTALLATION ONLY
I_{IN}, V_{OUT} AT SGA OUTPUT ONLY

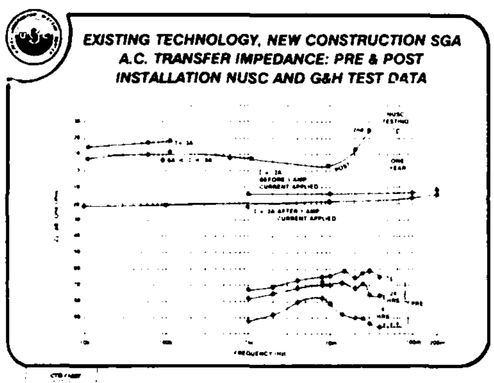

Existing Technology SGA:

- Variation in matter of hours.
- Nominal performance degradation with time ≈ 110 dB wide range.
- Spring technology showed performance varied with current.
- Nominal final performance + 10 dB//1 Ω.
- G & H test data (post-installation) showed:
  - Improved performance due to shipping.
  - Performance varies with magnitude of I.

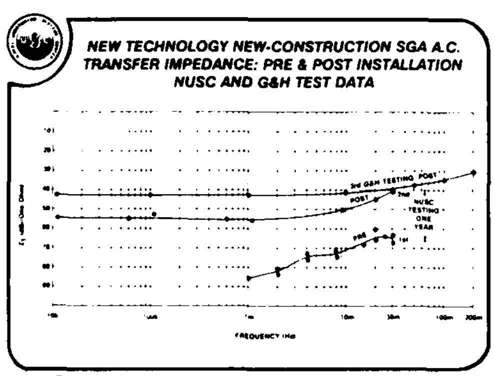

New Smart-Soldered Technology:

- Much less variation in performance-vs- time -- nominally 40 dB.
- No performance change with current changes.
- Nominal final performance -- -55 dB//1 Ω.
- G & H (post-installation) testing showed:
  - Reduced performance.
  - Performance change due to shipping.

G & H TEST RESULTS OF VARIOUS SGA SAMPLES

COMPARISON OF TRANSFER IMPEDANCE TEST DATA FOR THREE TYPES OF RG-214 STYLE SGA'S

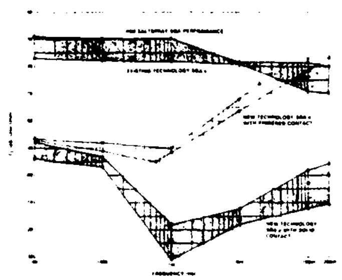

- Samples of various SGA's.
- Two bottom curves illustrate initial fingered contactor and final solid contactor.
- Top curve illustrates several spring technology SGA's.
- Performance level typical after days.

CONCLUSIONS AND RECOMMENDATIONS

CONCLUSIONS

- D.C. SGA (ONLY) PERFORMANCE IMPROVED (SLIGHTLY) WITH TIME FOR BOTH
- LONG TERM D.C. PERFORMANCE DOMINATED BY SGA-TO-KICKPIPE THREAD RESISTANCE
- SPRING CONTACT SGA PERFORMANCE IMPROVED BY "RE-TORQUING"
- SPRING TECHNOLOGY (EXISTING) SGA A.C. PERFORMANCE DIRECTLY RELATED TO SHIELD CURRENT (↑I, ↑ PERFORMANCE)
- SGA PERFORMANCE-VS-TIME
  - SPRING TECHNOLOGY: -96 TO +24 = 120 dB DEGRADATION
  - SMART SOLDERED TECHNOLOGY: -85 TO -41 = 44 dB DEGRADATION
- THREAD IMPEDANCE AT KICKPIPE INTERFACE DOMINATES LONG TERM SGA "SYSTEM" PERFORMANCE
- LIFE CYCLE PERFORMANCE OF EMC/EMP DEVICES MUST BE CONSIDERED
- EMI MODELING IMPROVED SGA PERFORMANCE BY 35 dB
  - EARLY FINGERED SHIELD CONTACTOR
  - FINAL "SOLID" SHIELD CONTACTOR

RECOMMENDATIONS

- DEVELOP EMI MODEL TO EVALUATE/PREDICT THREAD DEGRADATION
- DEVELOP SOLUTION TO THREAD DEGRADATION:
  (1) SHORT TERM: ELECTROCHEMICAL?
  (2) LONG TERM: MECHANICAL REDESIGN?
- DEVELOP PERFORMANCE VICE CONSTRUCTION BASED SGA SPECIFICATION
- DEVELOP TEST PROCEDURE THAT ENSURES ACCURATE & REPEATABLE TEST RESULTS
- INSTALL LATEST SGA & THREAD SOLUTION RECOMMENDATION ON TEST PLATFORM
- REMOVE SOLID SHIELD CONTACTOR SGA WITH SILVER CONDUCTIVE GREASE FROM TEST PLATFORM TO EVALUATE EXPECTED THREAD DEGRADATION
- EVALUATE SGA PERFORMANCE REQUIREMENT BASED ON SYSTEM APPROACH

SECTION 2

DEVELOPMENT OF A FULL PERFORMANCE COMPOSITE CONNECTOR WITH LONG TERM EMI SHIELDING PROPERTIES

DEVELOPMENT OF A FULL PERFORMANCE COMPOSITE CONNECTOR WITH LONG-TERM EMI SHIELDING PROPERTIES

by
Maurice Avoux
formerly of G & H Technology, Inc.,
Camarillo, CA, USA

David S. Dixon, Member IEEE
Naval Underwater Systems Center, New
London, CT, USA

James V. Masi, Member IEEE
Department of Electrical Engineering
Western New England College, Springfield,
MA, USA

HIGH TEMPERATURE THERMOSET AND THERMOPLASTIC RESINS

*MIL-C-38999, SERIES IV

*MIL-C-28840

1.	(PEEK)	POLYETHERETHERKETONE	282°C	(540°F)
2.	(LCP)	LIQUID CRYSTAL POLYMER - (XYDAR)	240°C	(464°F)
3.	(PPS)	POLYPHENYLENE SULFIDE (RYTON)	232°C	(450°F)
4.	(PAI)	POLYAMIDEIMIDE (TORLON)	220°C	(428°F)
5.	(PI)	POLYIMIDE	204°C	(399°F)
6.	(PES)	POLYETHERSULFONE	180°C	(356°F)
7.	(PAS)	POLYARYLSULFONE	180°C	(356°F)
8.	(PEI)	POLYETHERIMIDE (ULTEM)	180°C	(356°F)

*CONTINUOUS USE TEMPERATURE REQUIREMENTS:

MIL-C-38999, SERIES IV-175°C (347°F)

MIL-C-28840 - 200°C (392°F)

Three factors are prime in the determination of the behavior and properties of composites, both from a mechanical and electrical point of view, exclusive of the approach:

1. The fundamental materials of which the composite is composed;
2. the morphology and structural disposition of the constituents; and
3. The multifactorial interaction among the constituents (e.g. chemical, mechanical, and electrical).

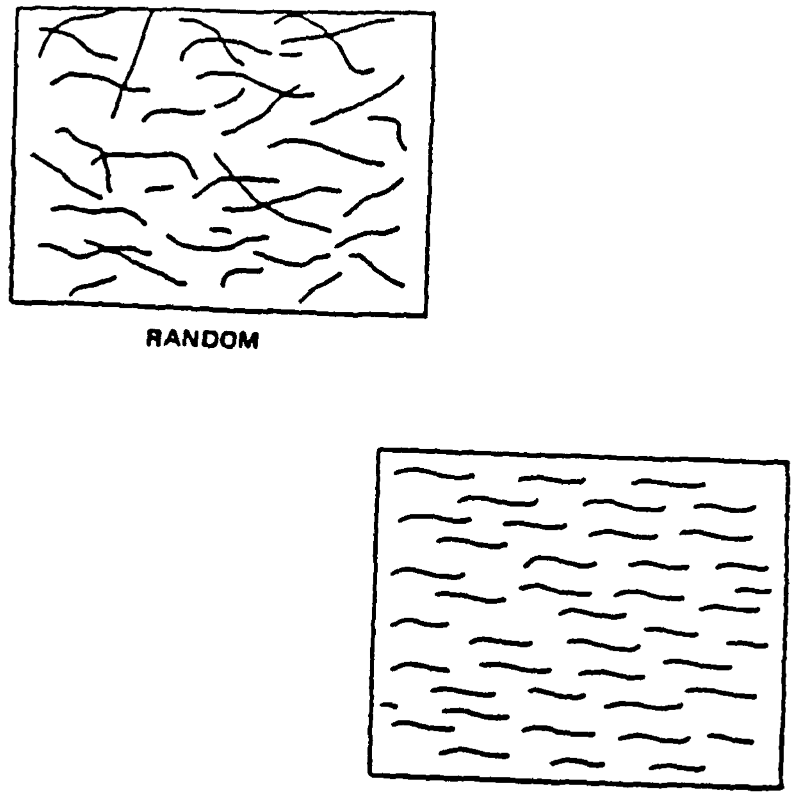

Orientation of fibers.

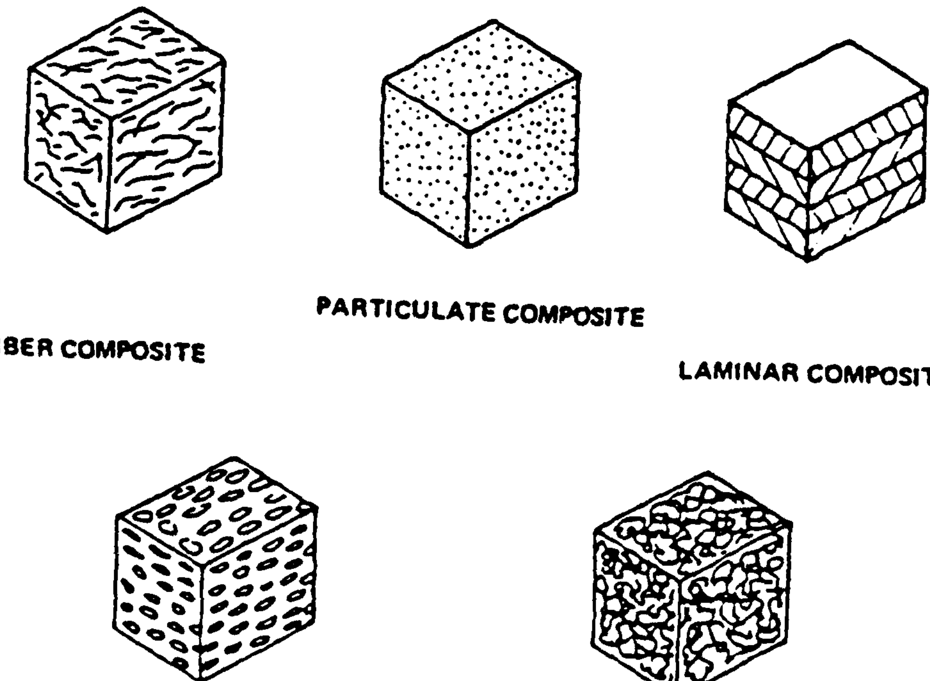

Classes of composites.

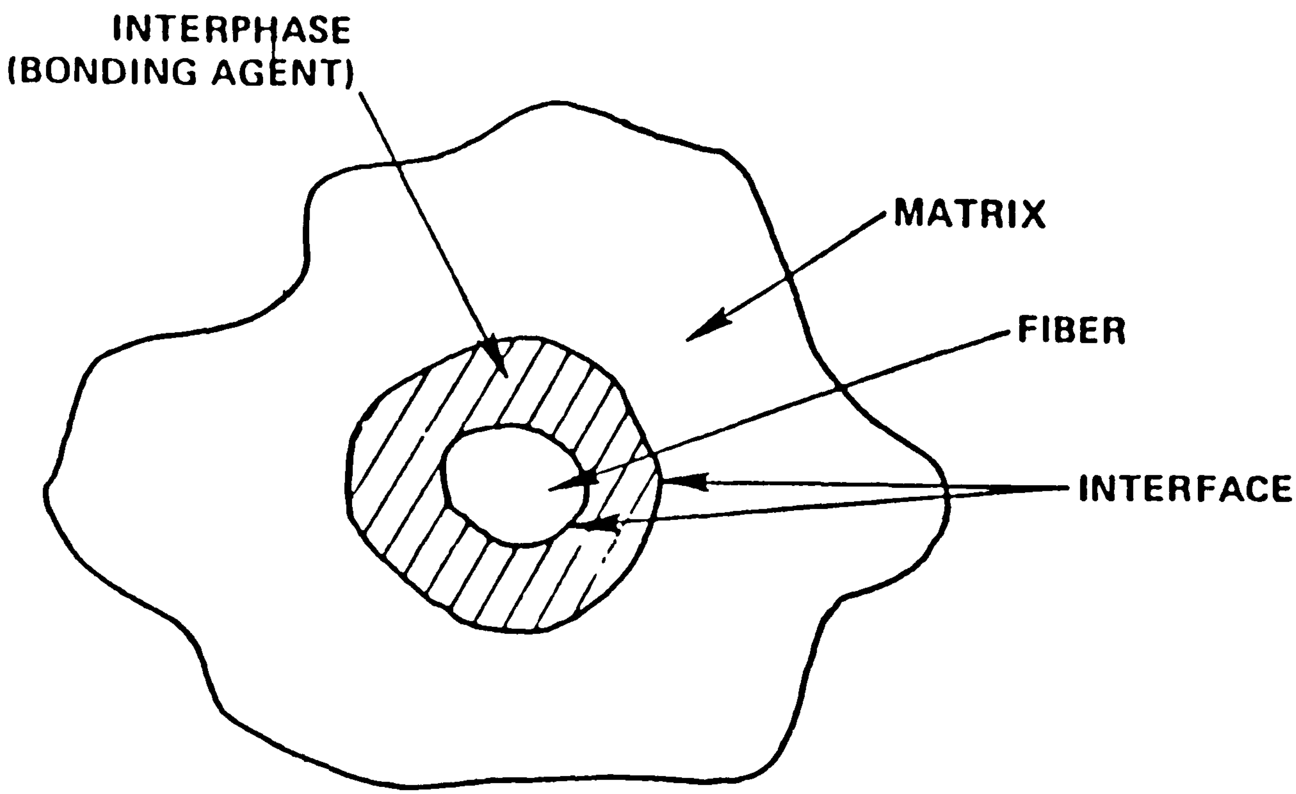

Makeup of interface between fiber and matrix.

the Halpin-Tsai equation is:

(1) Tensile: $E_c = V_f E_f + V_m E_m$, and

(2) Transverse: $E_c = [(1 + 2\eta V_f)/(1 - \eta V_f)] E_m$,

where

$\eta = \{[(E_f/E_m)-1]/[(E_f/E_m)+2]\}$,

E_c is the modulus of the composite, E_f and E_m are the moduli of the filler and the matrix, respectively, and V_f and V_m are the volume fractions of the filler and matrix, respectively. These are the approximate bases on which the mechanical properties of the ideal composite were pre-estimated.

TENSILE PROPERTIES (ASTM D-63
15 w/o PEEK COMPOSITES

PROP.	InSnOx	Graphite	PEEK
Strain @ break	1.56%	2.1%	3.9%
Stress @ break	19.94Ksi	14.57Ksi	13.4Ksi
Elast mod.	1.37Msi	1.38Msi	1.27Msi

Injection molded samples: parallel to flow axis.

InSnOx (particles), Graphite (fibers)

SURFACE RESISTIVITY SPECTRUM

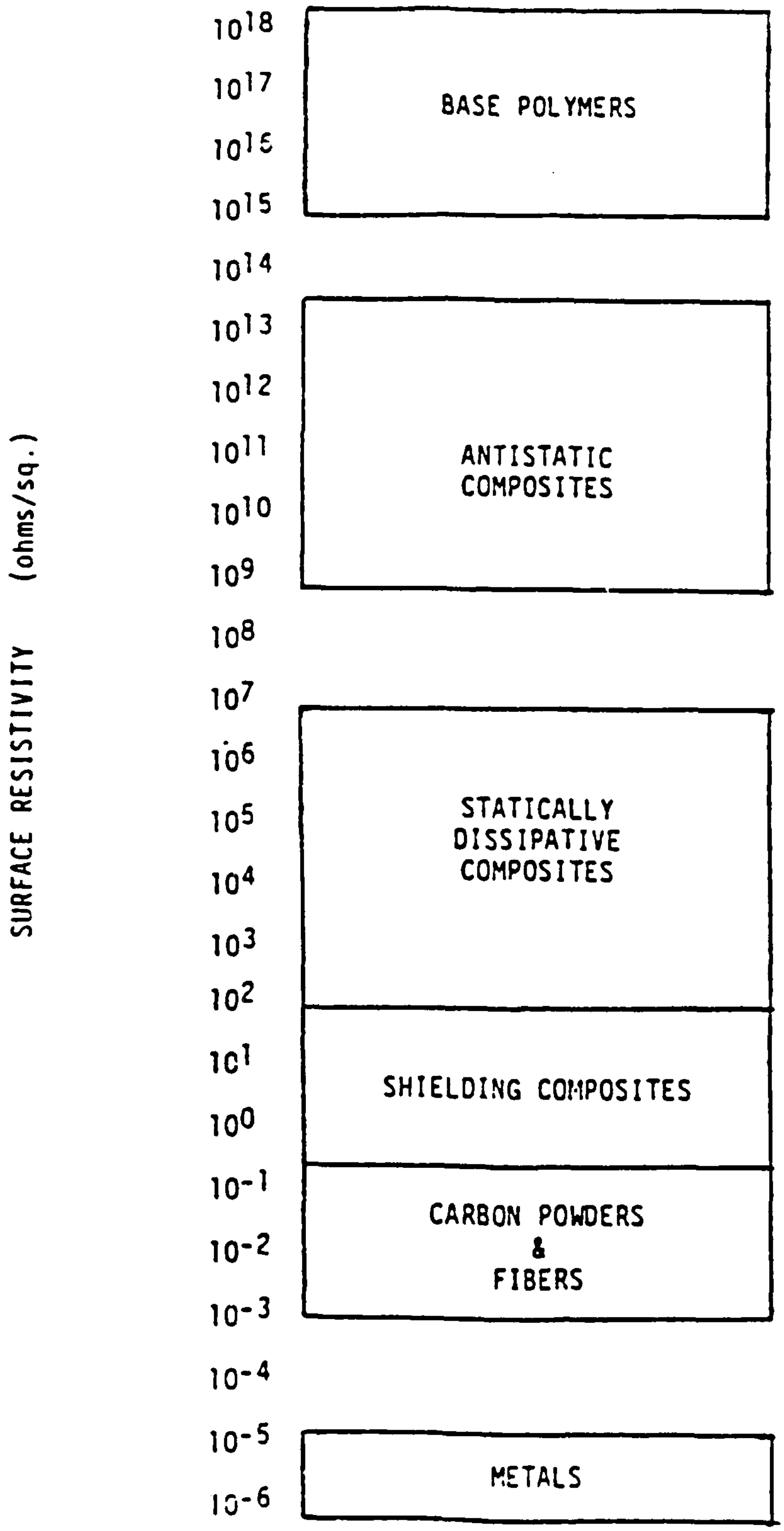

Applying the effective medium theory[12] to the conductivity and the complex dielectric constant of the composite material, one can obtain a relationship between the properties of the matrix and those of its components by

$$V_f(\varepsilon_f^* - \varepsilon_c^*)/(\varepsilon_f + 2\varepsilon_c^*) = -(1-V_f)(\varepsilon_m^* - \varepsilon_c^*)/(\varepsilon_m^* + 2\varepsilon_c^*) \,, \tag{5}$$

where

$$\varepsilon_f^*,\ \varepsilon_m^*,\ \text{and}\ \varepsilon_c^*$$

are the complex dielectric constants of the filler, matrix, and composite, respectively, and V_f is the volume fraction of the filler.

In general,

$$\varepsilon^{*} = \varepsilon_{r} - j\sigma / \varepsilon_{o}\omega \qquad (6)$$

Applying the effective medium theory[12] to the conductivity and the complex dielectric constant of the composite material, one can obtain a relationship between the properties of the matrix and those of its components by

$$(5) \qquad V_f(\varepsilon_f^* - \varepsilon_c^*)/(\varepsilon_f + 2\varepsilon_c^*) =$$

$$-(1-V_f)(\varepsilon_m^* - \varepsilon_c^*)/(\varepsilon_m^* + 2\varepsilon_c^*) \ ,$$

where

ε_f^*, ε_m^*, and ε_c^*

are the complex dielectric constants of the filler, matrix, and composite, respectively, and V_f is the volume fraction of the filler.

expression for penetration depth:

$$d = \frac{\lambda_o}{\pi}\left(\frac{1}{2\epsilon'[(1+\tan^2\delta)^{\frac{1}{2}} - 1]}\right)^{\frac{1}{2}}$$

where d = penetration depth (power)

λ_o = wavelength in free space

ϵ' = dielectric constant

$\tan\delta$ = loss tangent

EQUIVALENT CIRCUIT

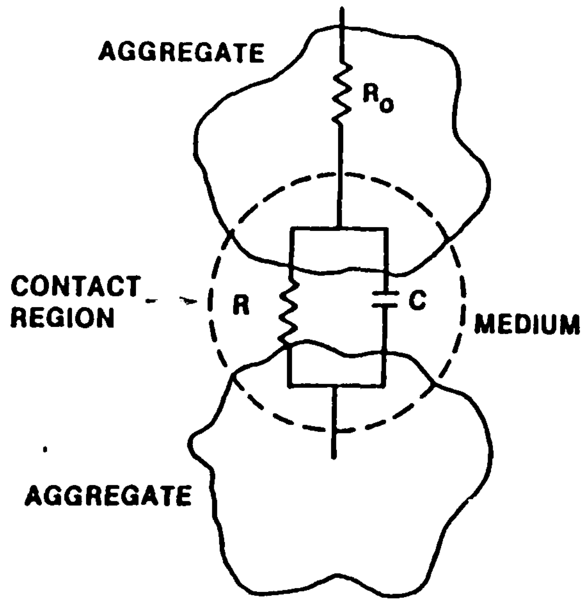

CTS-11013

Using the form factors for the particle, flake, or fiber involving cross-sectional area considerations of the filler (A), inter-fiber/flake/particle spacing (d), frequency ϵ, resistivity (ρ) as in equation (3), the impedance of the specimen can be expressed by

$$(7) \quad Z = -j/[\rho\,(\epsilon_0 \epsilon_r A/d) - j(A/\rho_p d)] + R_0.$$

MEASURED IMPEDANCE-VS-FREQUENCY FOR CYLINDRICAL SAMPLE OF GRAPHITE IN POLYCARBONATE (@.1V)

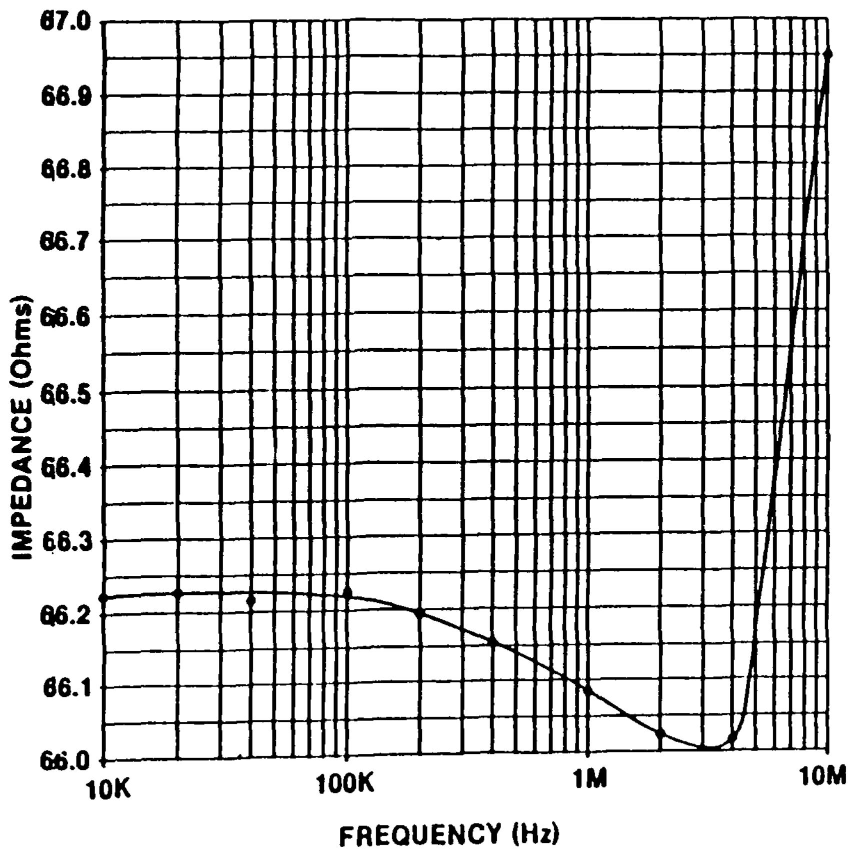

CTS-11015

MEASURED IMPEDANCE-VS-FREQUENCY FOR RECTANGULAR SAMPLE OF GRAPHITE IN POLYCARBONATE (@.1V)

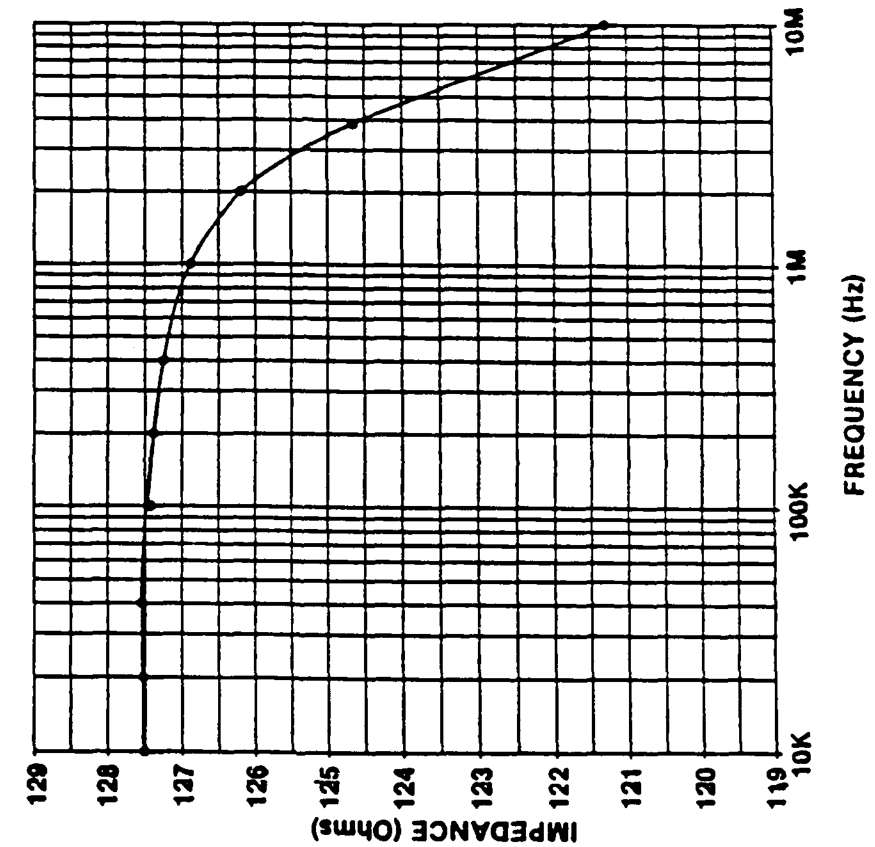

CTS-11016

DIRECT SE MEASUREMENTS

STANDARD METHODS

- ASTM ES7-83
- NBS METHOD
- MILITARY STANDARDS 285, 461/462-B
- FCC TESTING

METHODS VARY AMONG VARIOUS INDUSTRIES

METHODS OF ANALYSIS
Z AND COMPLEX PERMITTIVITY

- IMPEDANCE BRIDGE (100-1E7 Hz)
- ADMITTANCE BRIDGE (1E7-1E9 Hz)
- NETWORK ANALYZER (4E6-1.5E9 Hz)
  MOD. TYPE-N CONNECTOR
  "BUTTON" MOD. IN-LINE COAX.
  BEADLESS COAX. AIRLINE
  ASTM COAX.
- PRELIMINARY THEORY
- WHY IMPEDANCE? WORKS FOR BOTH
  METAL AND COMPOSITE.

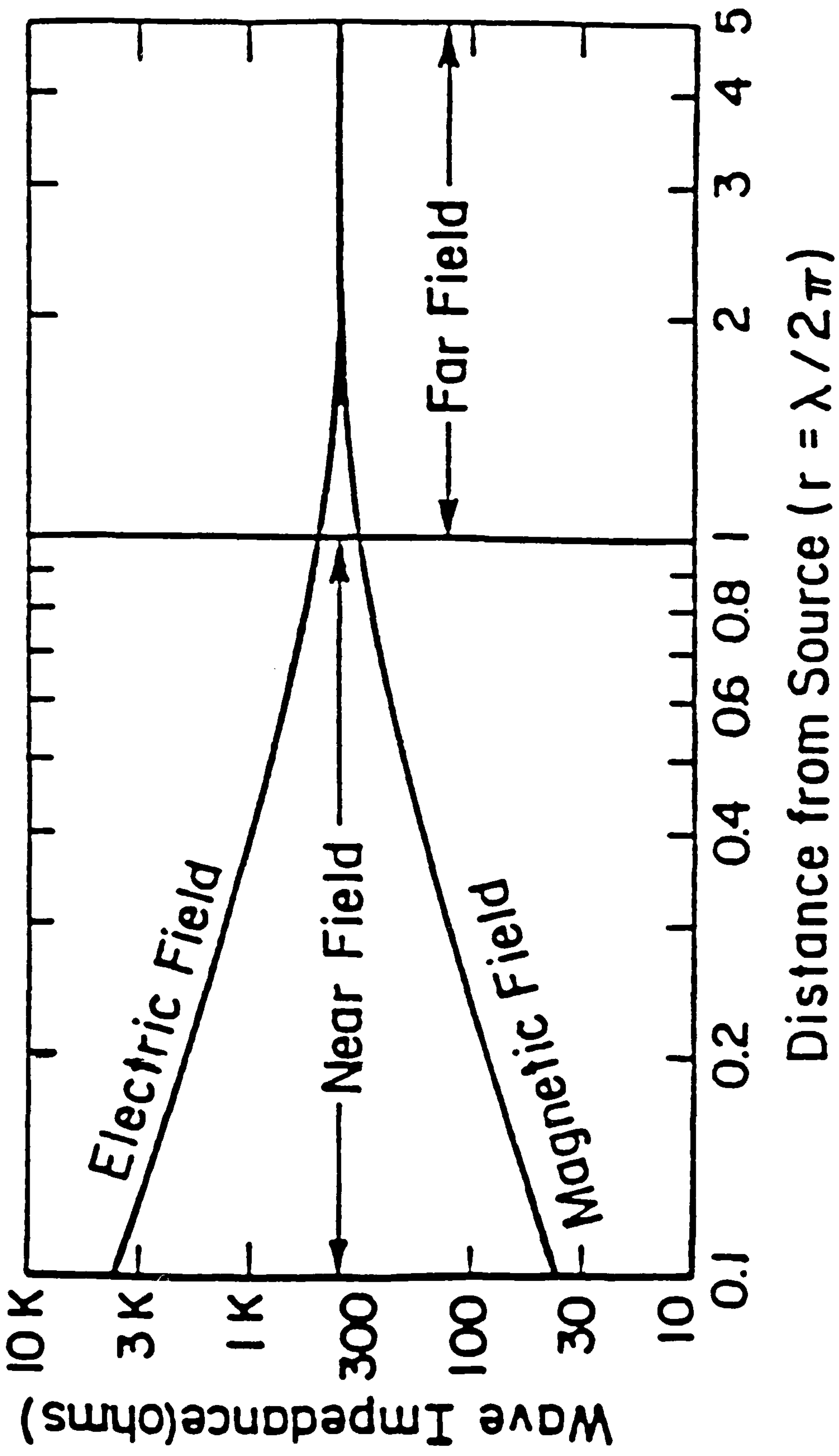
Wave Impedance(ohms)
10 K
3 K
1 K
300
100
30
10
0.1
0.2
0.4
0.6
0.8
1
2
3
4
5
Distance from Source (r = λ/2π)
Electric Field
Near Field
Magnetic Field
Far Field

Functionally, the equivalent circuit can be expressed as a series combination of resistance and inductance with a parallel combination of resistance and capacitance:

$$Z = R_s + (d/2\pi f \epsilon_o \epsilon'_r A)[\tan \delta/(\tan^2\delta + 1)]$$

$$+ j\,[(2f\mu_o l \cosh^{-1}(d/4D)) - (d/2\pi f \epsilon_o \epsilon'_r)/(\tan^2\delta + 1)$$

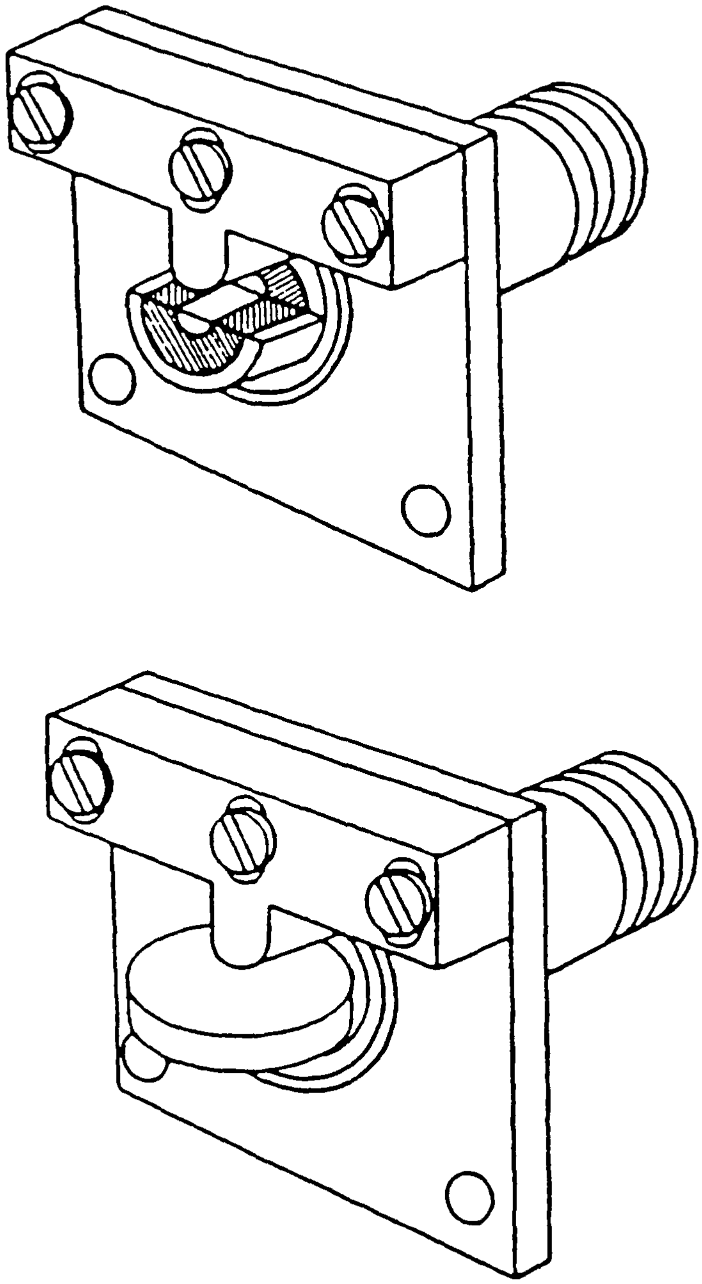

a: N type connector modified for use in the reflection-coefficient measurement of carbon-plastic samples. b: A button-shaped sample mounted in the N-type connector.

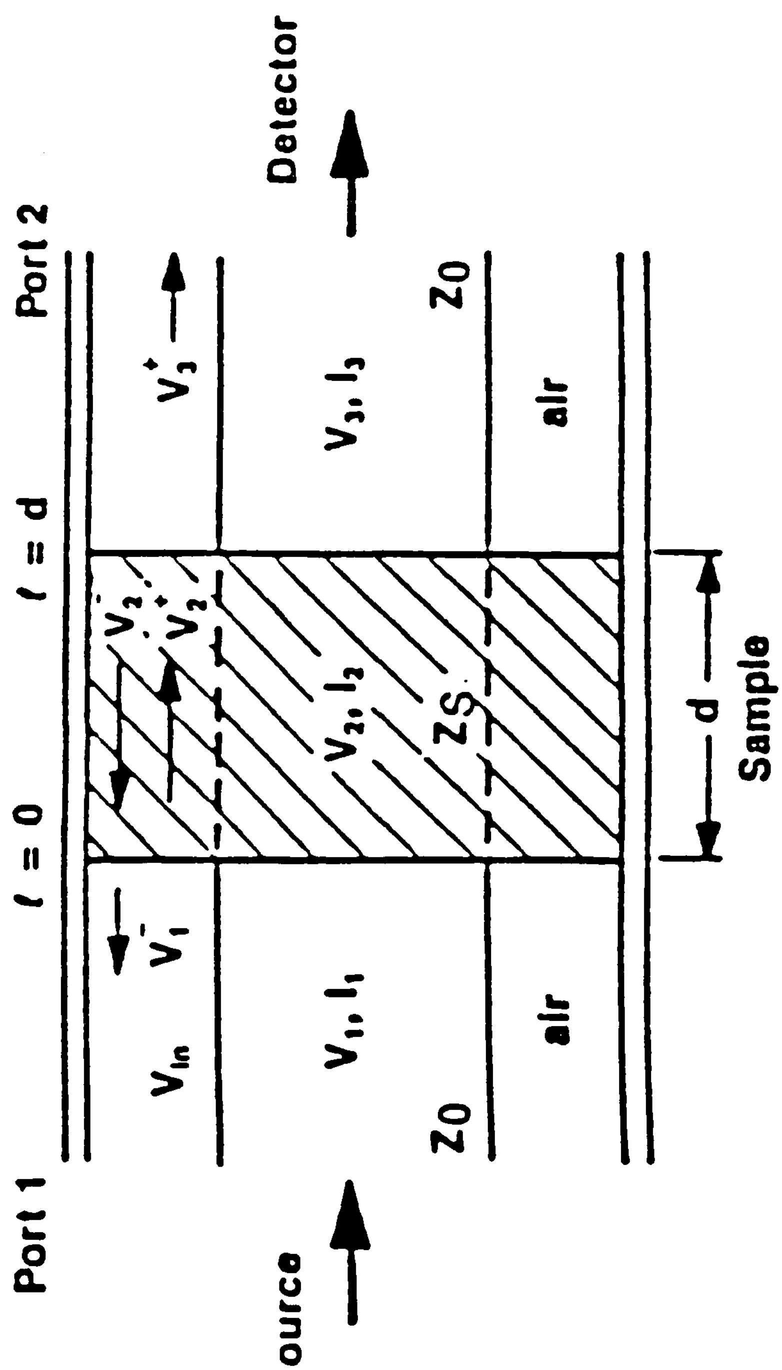

Air Line with Filled Material.

MATERIAL PARAMETERS - MEASUREMENT

REFLECTION AND TRANSMISSION MEASUREMENT
ALLOWS DETERMINATION OF ABSORPTION

- S-PARAMETERS MEASURED VIA HP-8510 NETWORK ANALYZER
- DETERMINATION OF μ_r^* & ϵ_r^*
- PROVIDES MORE DATA THAN IS COMMONLY USED BY INDUSTRY FOR MATERIAL EVALUATIONS

Coaxial Measurement Setup

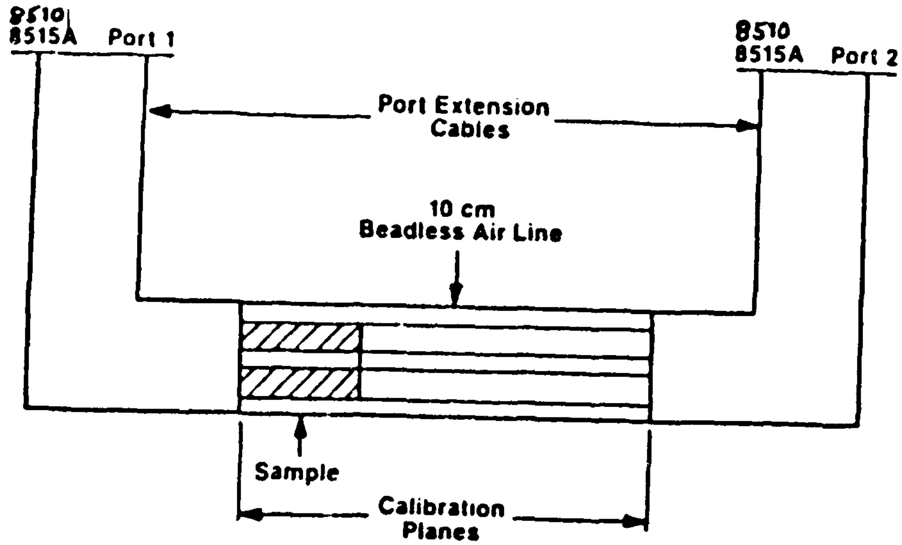

Coaxial Sample Holder
(10 cm APC-7 Beadless Air Line)

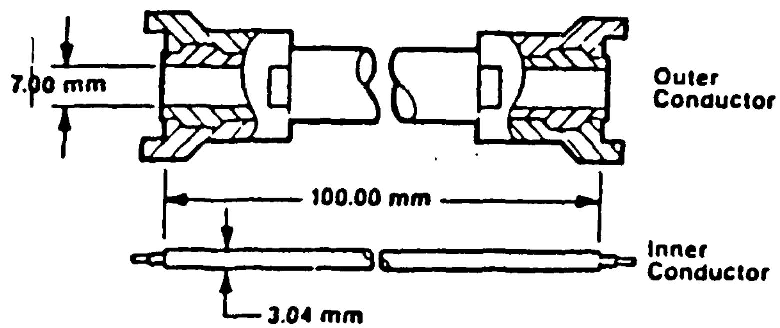

$$S_{11}(\omega) = \frac{(1 - T^2)\,\Gamma}{1 - T^2\Gamma^2} \qquad [1]$$

$$S_{21}(\omega) = \frac{(1 - \Gamma^2)\,T}{1 - T^2\Gamma^2}$$

Where Γ is the reflection coefficient between Z_0 and Z_S when the length of materials is infinite ($l = \infty$); and

$$\Gamma = \frac{Z_S - Z_0}{Z_S + Z_0} = \frac{\sqrt{\frac{\mu_r}{\varepsilon_r}} - 1}{\sqrt{\frac{\mu_r}{\varepsilon_r}} + 1} \qquad [2]$$

The term T is the transmission coefficient in the materials (of finite length) and can be written:

$$T = \exp\left(-j\omega\sqrt{\mu \cdot \varepsilon} \cdot d\right) = \exp\left[-j(\omega/c)\sqrt{\mu_r \cdot \varepsilon_r} \cdot d\right] \qquad [3]$$

Equation [1] allows Γ and T to be derived by measuring $S_{11}(\omega)$ and $S_{21}(\omega)$. These quantities can then be used to calculate the complex permittivity (ε_r) and permeability (μ_r).

FLANGED COAXIAL HOLDER

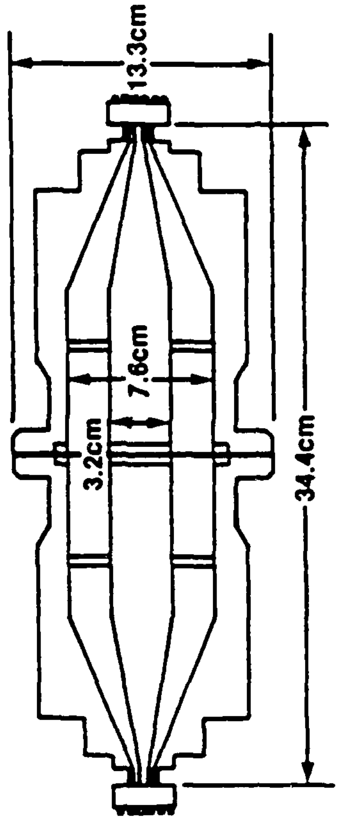

CTS-11010

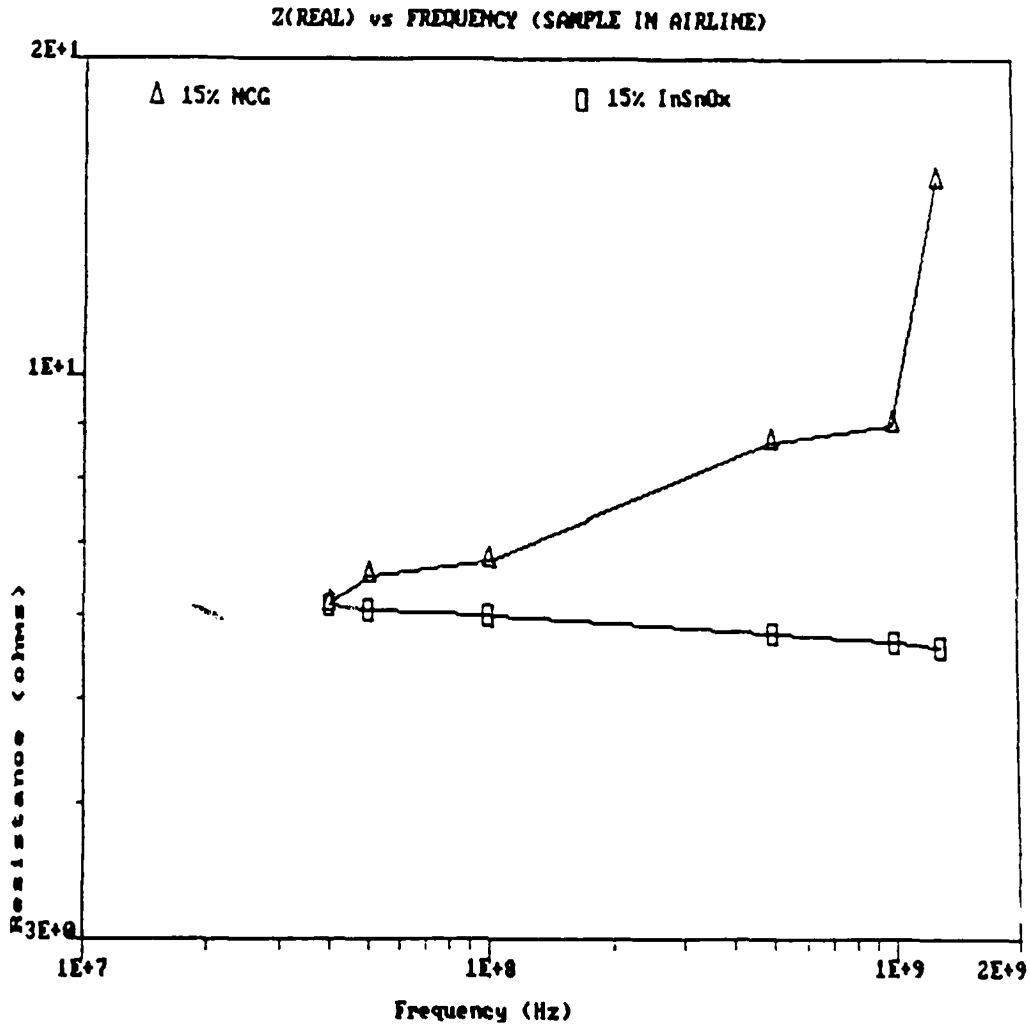
Z(REAL) vs FREQUENCY (SAMPLE IN AIRLINE)
Δ 15% NCG
□ 15% InSnOx
2E+1
1E+1
3E+0
Resistance (ohms)
1E+7
1E+8
1E+9
2E+9
Frequency (Hz)

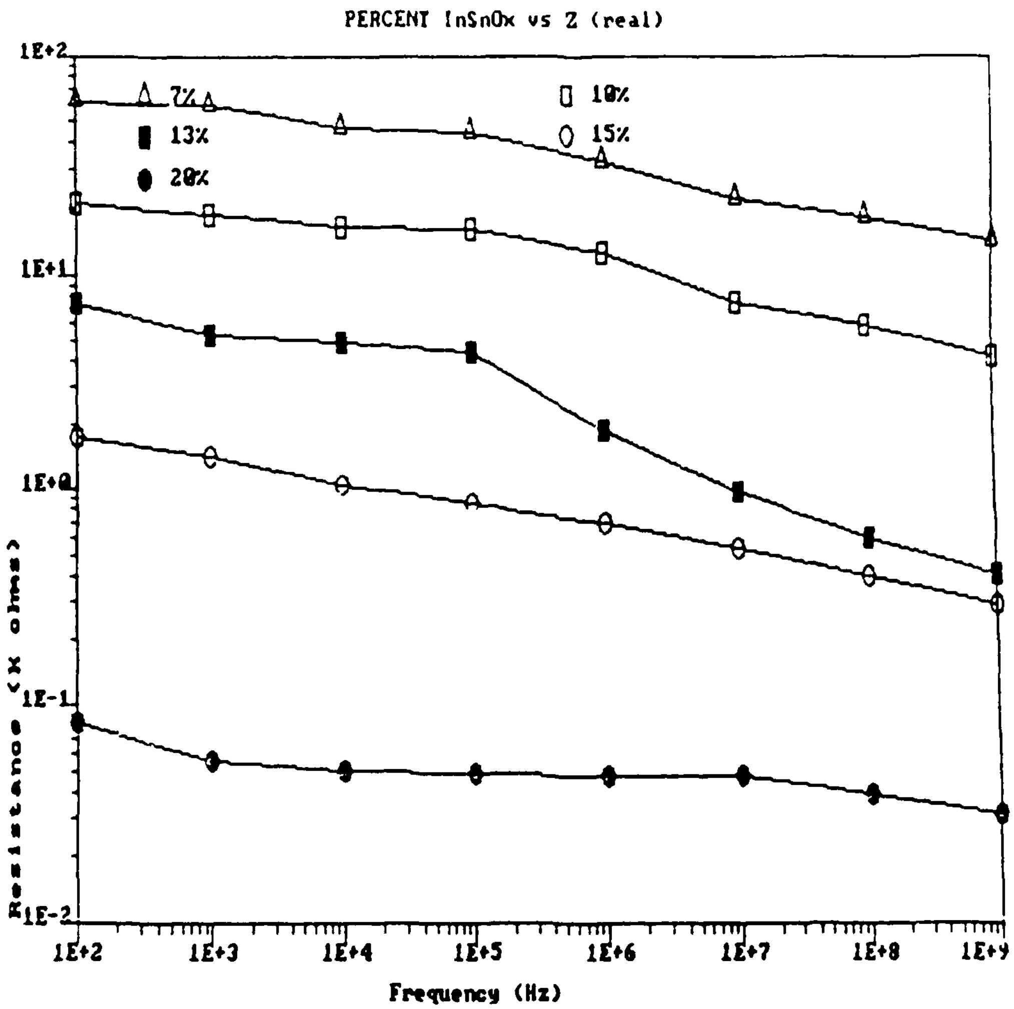
PERCENT InSnOx vs Z (real)
7%
10%
13%
15%
20%
1E+2
1E+1
1E+0
1E-1
1E-2
Resistance (K ohms)
1E+2
1E+3
1E+4
1E+5
1E+6
1E+7
1E+8
1E+9
Frequency (Hz)

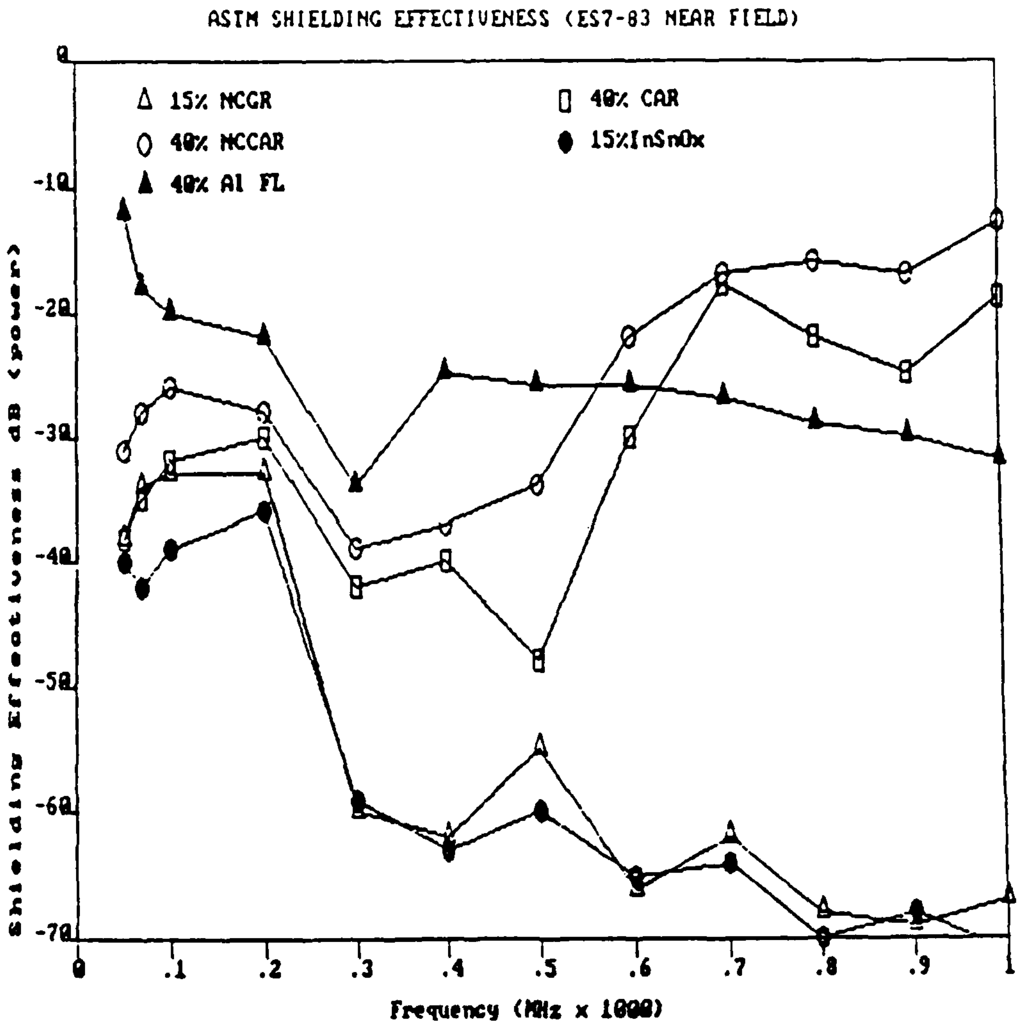
ASTM SHIELDING EFFECTIVENESS (ES7-83 NEAR FIELD)
15% NCGR
40% CAR
40% NCCAR
15%InSnOx
40% Al FL
Shielding Effectiveness dB (power)
0
-10
-20
-30
-40
-50
-60
-70
0
.1
.2
.3
.4
.5
.6
.7
.8
.9
1
Frequency (MHz x 1000)

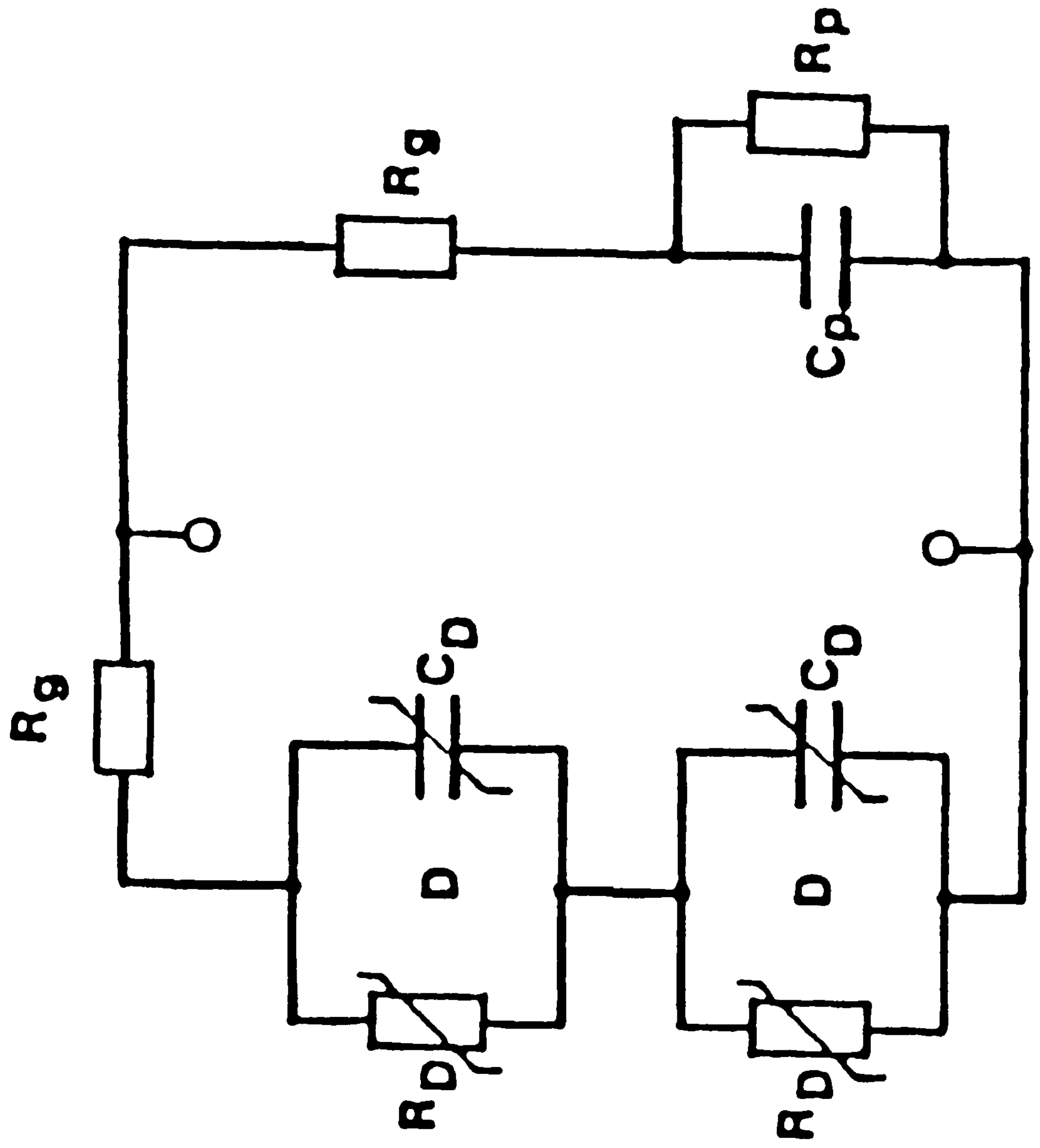

equivalent circuit

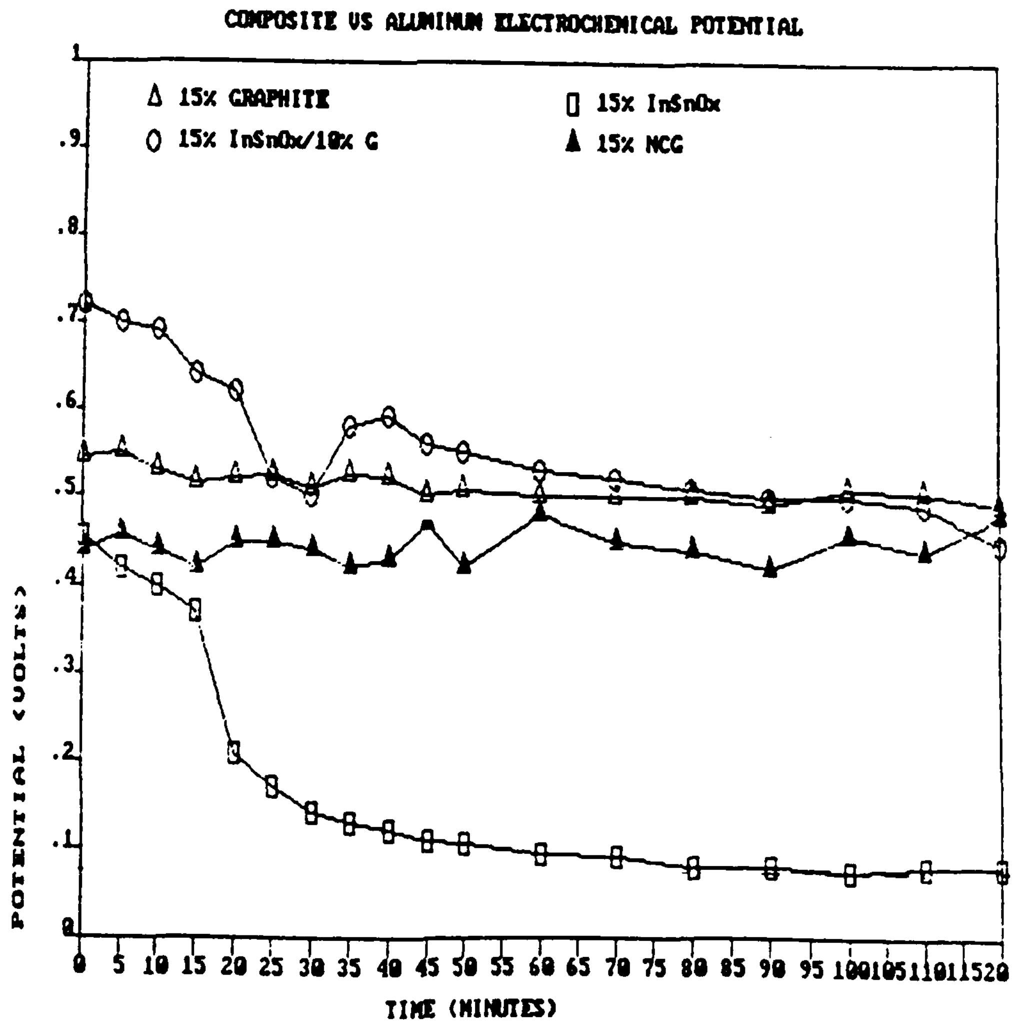
COMPOSITE VS ALUMINUM ELECTROCHEMICAL POTENTIAL
Δ 15% GRAPHITE
○ 15% InSnOx/10% G
□ 15% InSnOx
▲ 15% NCG
POTENTIAL (VOLTS)
TIME (MINUTES)

```
Start Freq =      1000
Stop Freq  =       50000

particle = sphere
dia:     0.000100000
spacing:0.000000010

Rho = 0.00100

Restance = 160.000000000 Ω
Area     = 0.000000008

sigma polymer σ= 0.000000100

Epsilon R' =  25.00
Epsilon R"=   0.10

F1: Edit     F2: Plot     F3: Plot     F4: Plot     F5: Exit
    Param         Real         Imag        Phase      to DOS
```

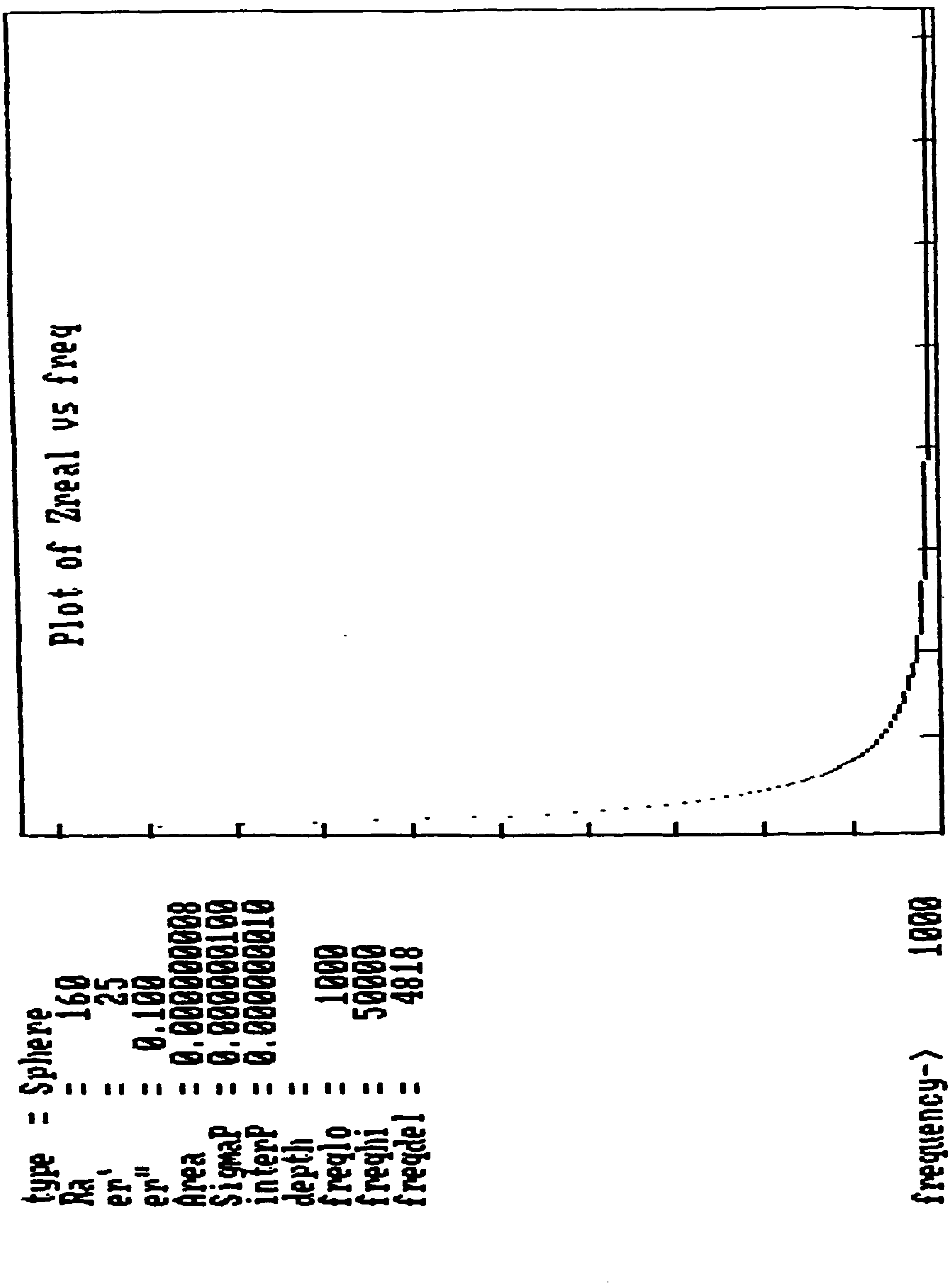
Plot of Zreal vs freq
type = Sphere
Ra = 160
er' = 25
er" = 0.100
Area = 0.0000000008
SigmaP = 0.0000000100
interP = 0.0000000010
depth =
freqlo = 1000
freqhi = 50000
freqdel = 4818
frequency-> 1000

APPENDIX A

AN EVALUATION OF THE LONG TERM EMI PERFORMANCE OF SEVERAL SHIELD GROUND ADAPTERS

An Evaluation of the Long Term EMI Performance of Several Shield Ground Adapters

DAVID S. DIXON, MEMBER, IEEE, and STANLEY I. SHERMAN, MEMBER, IEEE

Naval Underwater Systems Center
New London Laboratory (NUSC/NLL)
New London, CT 06320

and

MICHAEL VAN BRUNT
G & H Technology, Inc.
750 W. Ventura Bvd.
Camarillo, CA 93010

ABSTRACT

A shield ground adapter (SGA) is a device utilized to establish a 360° low impedance electrical connection between a cable's shield and the ground structure through which the cable passes. This low impedance connection is designed to reduce and/or eliminate EMI and/or EMP problems by shunting high level currents into the systems' ground plane. This paper will discuss the measured EMI performance characteristics of an existing (spring) technology SGA and a new technology SGA that utilizes a recently developed smart-soldering technique and an improved cable shield-to-SGA connection method. Over one year ago, one new construction model of each SGA was installed on the deck of a U.S. naval ship. This paper will discuss the a.c. and d.c. EMI measurements that were conducted on the SGAs. The measurements were conducted both before the installation and one year later, after being exposed to 12 months of a harsh marine environment.

BACKGROUND

A metallic boundary is typically established by EMI and EMP personnel to protect electronic equipment from high level electromagnetic fields. These fields can be created in peacetime by lightning and nearby communication transmitters or in times of conflict by an Electromagnetic Pulse (EMP). In certain instances it is necessary to have shielded signal cables transition this metallic boundary. It is estimated that over 80 dB of attenuation is required at such interfaces to reduce the hundreds of amperes of current that could be flowing on cable shields. One method of preventing electronic system damage is to shunt these currents into the system ground plane at the point where these cables pass through the grounded metallic boundary. This can be accomplished by employing devices referred to as Shield Ground Adapters (SGAs). This type of protection may be required at the topside-to-below decks interface of a ship or the external-to-internal interface of a building, or the compartment-to-compartment interface between isolated below-decks spaces.

Early EMC work on FFG-7 Class platforms indicated that EMI energy was being coupled into below-decks areas by currents flowing on cable shields. These currents were producing below-deck environmental levels exceeding the "normal" environmental levels assumed by MIL-STD-461 for electronic equipments. Initial efforts to reduce these below-deck field levels by grounding cable shields produced significant reduction of below-deck field strengths. These reductions came in spite of the temporary and unsophisticated nature of various grounding techniques initially utilized to connect the cable shield to the ship's hull. Military specifications [1] for electronic equipment now recommend the use of SGAs to reduce cable shield currents.

ENVIRONMENTALLY SEALED SGAs

EARLY SGAs

Figure 1 illustrates the evolution of cable shield grounding devices. The earliest environmentally sealed SGAs utilized ballpoint pen style springs that were connected end-to-end around the signal cable's shield. These springs were then compressed against the signal cable's shield to shunt EMI currents into the system or platform ground plane. This type of SGA utilizes a spring member that encircles the shield of a typical R.G. cable. This spring member is then mechanically compressed when assembled. The operational performance of this grounding device is directly related to the contact force between the shield and the spring member. The essence of this type of device is maintaining a certain amount of contact force that yields a certain level of transfer impedance (Zt). There exists several modes that can and do degrade the performance of these devices. The level of performance (Zt) is directly related to the contact force between the shield and the spring member. Typical shipboard cables such as R.G. 214 have a dielectric inner, which can cold flow due to excessive compressive force of the grounding spring. If this cold flow phenomenon takes place, the contact force between cable shield and spring contact will change, possibly affecting the performance of the signal being transmitted along the cable.

It was suspected that the EMI/EMP performance of this compression type of SGA would deteriorate with both time and environmental influences due to its spring-to-shield pressure method of achieving the necessary 360° contact between the cable shield and the system (or shipboard) ground plane. The suspected problems with this type of pressure sensitive shield contact became the basis for the Navy investing in research and development into the grounding of shielded cables and conduit.

Reference 2 delineated the short-term performance loss that was measured for an existing spring compression technology SGA. The SGA's performance deterioration after 6 hours ranged from 8 to 22 dB, over the frequency range from 1 MHz to 40 MHz. This performance loss increased with time such that after 24 hours the performance loss ranged from 13 to 34 dB.

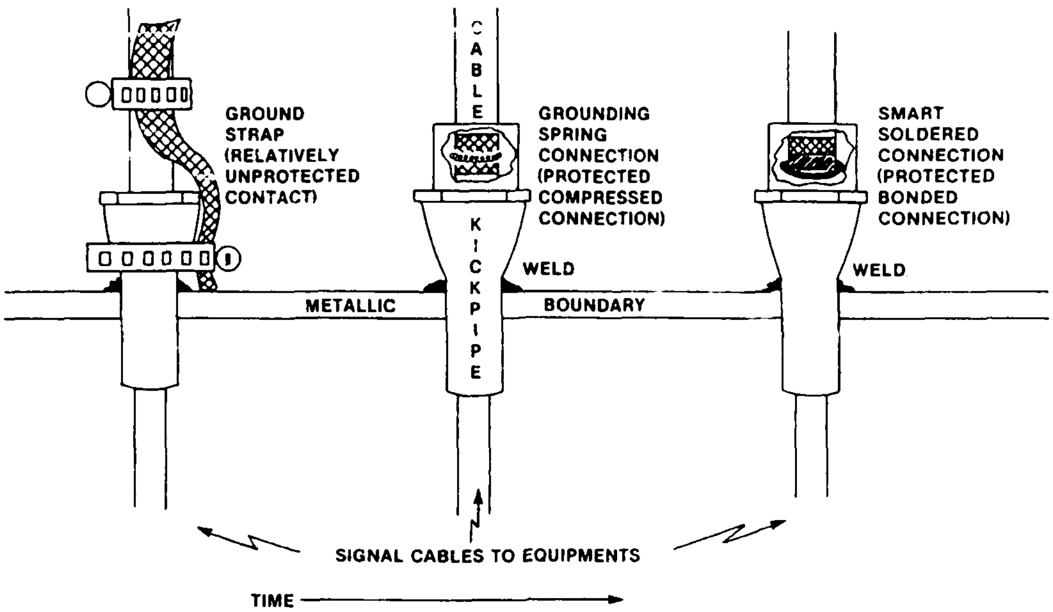

Figure 1: Cable Shield Ground Evolution

NEW TECHNOLOGY SGA

In a combined effort between the Naval Underwater Systems Center (NUSC), G & H Technology Inc. (G & H), and the University of Pennsylvania (UPENN), an improved SGA has been developed that will maintain a higher level of performance over the lifetime of the SGA, even after being exposed to hostile marine environments. This improvement is due to the utilization of a new method of bonding the cable grounding contact to the cable shield and to the development of an SGA that will connect the grounding contact to the system/platform ground. This new grounding contact is attached to the cable shield by soldering it to the shield utilizing a METCAL developed self-regulating temperature source (SR/TS) with their solder strap connection system [3]. Utilizing this technique, soldering temperatures are accurately maintained at levels high enough to provide an excellent solder bond between the grounding contact and the cable shield, but low enough to prevent any change in the cable's transmission characteristics. A paper by Van Brunt [4] discussed the mechanical design aspects of this new technology SGA.

NEED FOR LONG-TERM SGA PERFORMANCE EVALUATION

In order to evaluate the long-term performance of both existing and new technology SGAs, a new construction model (solid version vice retrofit split version) of each was installed at the topside-to-below decks interface of an FFG-7 Class Frigate. This would expose both devices to the hostile topside environment of a surface ship for over one year. Pre and post installation d.c. and a.c. Zt measurements were conducted on each SGA at both NUSC and G & H. In addition, shipboard d.c. measurements were also conducted on each SGA after six months of exposure to the topside environment.

PERFORMANCE VALIDATION OF EXISTING & NEW TECHNOLOGY SGAs

METHODS OF A.C. PERFORMANCE EVALUATION

Two methods of evaluating SGA performance have been utilized during this SGA development effort:

1. The first test method used to evaluate the SGA performance utilized a shielded room to isolate the SGAs input from its output. This procedure measured input current I(in) and the SGA output voltage between the cable shield and the ground plane V(out). This produced a V(out)/I(in) ratio or a SGA transfer impedance, Zt, which was proportional to the SGA's performance.

2. The second test method utilized a triaxial test fixture where an internally mounted inconel current probe measured I(in), and an internal connection between the cable shield and the system ground provided V(out).

TRANSFER IMPEDANCE (Zt) TESTING WITH SHIELDED ROOM

As shown in figure 2, a shielded room at NUSC was utilized to conduct transfer impedance (Zt) measurements at frequencies up to 30 MHz. The shielded room was utilized to electromagnetically isolate the SGA input from its output. A high power wideband amplifier was used to drive approximately 4 amperes of V.L.F. and H.F. currents down the coaxial cable shield. The SGA output-side of the cable shield was terminated inside the shielded room by the 50 Ohm input circuitry of the spectrum analyzer. Because of the very low values of shield-to-ground output voltage V(out) being measured, careful attention was given to the test apparatus grounding configuration. To improve measurement sensitivity, all the high level "source" equipment were placed outside of the shielded room, and the low level output measurement equipment were placed inside the shielded room.

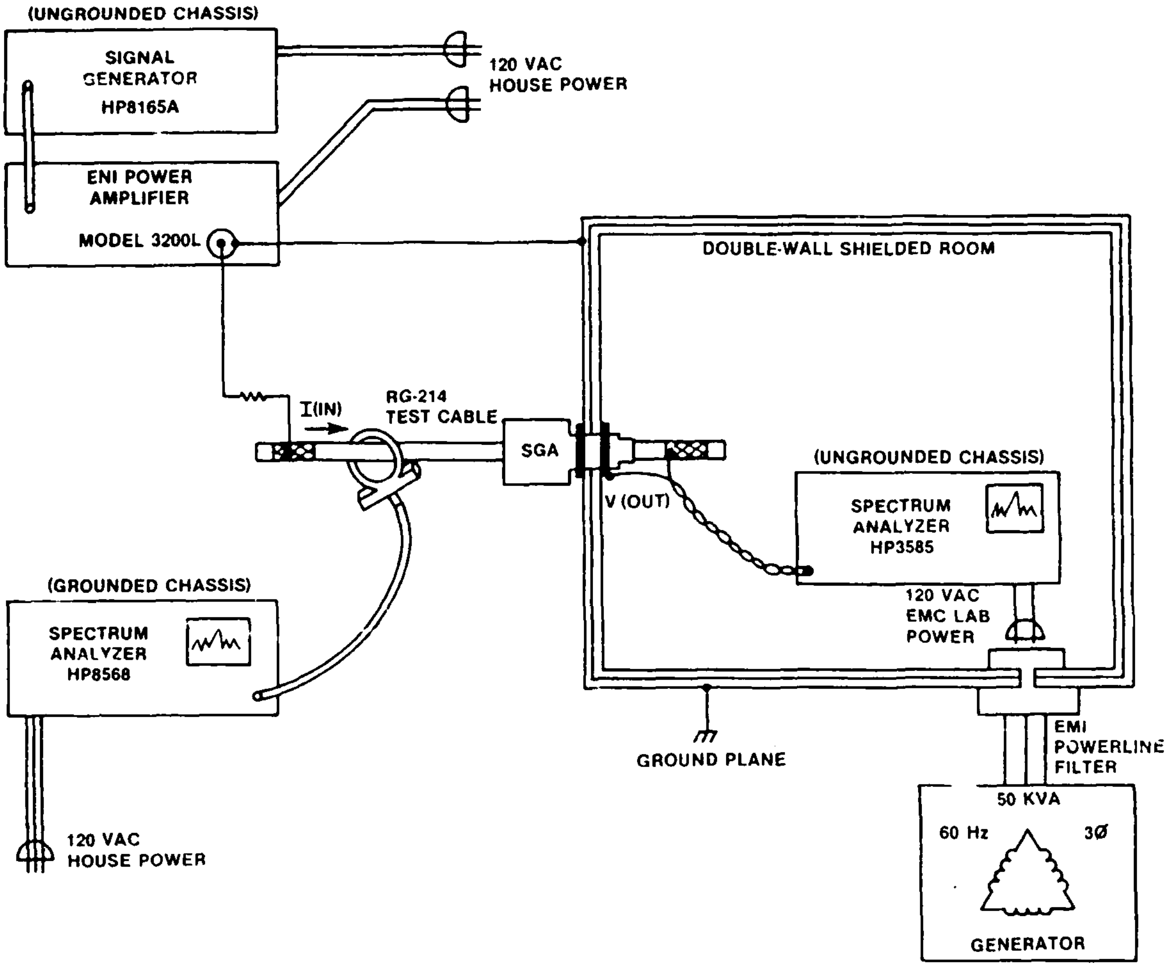

Figure 2: NUSC Transfer Impedance (Zt) Measurement Procedure Utilizing a Shielded Room

The SGA output shield-to-ground voltage being measured can be modeled as a voltage source with a series resistance equal to the contact resistance between the cable shield and the SGA. At most, this resistance is on the order of a few milli-Ohms. For testing purposes, this voltage is a good parameter to measure because it is inherently immune to all the cable variables associated with using a dual current probe measurement method. This measurement of performance is defined as V(out)/I1, and it can be seen that it has the units of impedance (Zt). This unit of performance is independent of the SGA installation, because the shield impedance at the SGA output will always be significantly more than the defined source impedance of the measured voltage; therefore, the configuration of the output side of the cable will have no significant effect on the V(out) measurement. Thus this V(out)/I(in) ratio provides a transfer impedance (Zt) value that is dependent on the effectiveness of the SGA shunt device and independent of output cable configuration.

TRIAXIAL TEST FIXTURE TRANSFER IMPEDANCE MEASUREMENT METHOD

A test fixture was constructed at G & H that would measure the SGA performance over an extended frequency range from 10 kHz to 200 MHz. The fixture shown in figure 3 was constructed to accomodate the termination of a shielded cable whose diameter was as great as that of a R.G. 319 rigid coax (2.5 inches). The fixture is a modified version of a MIL-SPEC triaxial fixture. It is basically operated in a shorted coax configuration with the input fed on one side of the short and the output taken on the other. The input is coaxial, externally loaded, and internally shorted, and an inconel current sensor is placed at the shorted end. The output section is coaxial, internally shorted, and externally loaded. The fixture resembles a stubb triax with the exception of the added current sensor. The sensitivity of this system is approximately 5 nano-Ohms.

COMPARISON OF Zt TEST DATA WITH PREDICTED (EMI MODEL) PERFORMANCE

For frequencies below 30 MHz, comparisons of transfer impedance test data were made between the triaxial measurement procedure and the shielded room measurement procedure. As shown in figure 4 this comparison of test data from the same new construction, fingered shield contactor SGA, yielded SGA transfer impedance (Zt) values that were within 4 dB of each other. This closeness in data occurred in spite of the fact that the SGA was tested using

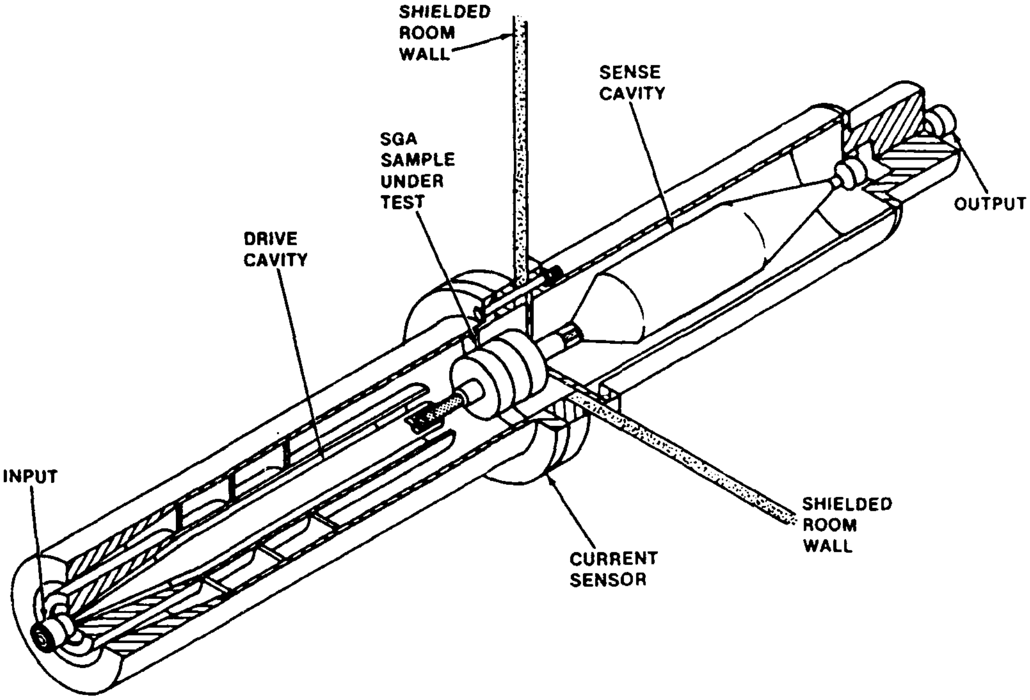

Figure 3: G&H Technology Transfer Impedance (Zt) Measurement Test Fixture

completely different: (1) measurement equipment, (2) personnel, (3) shielded rooms, (4) test procedures, and the data was measured almost two weeks apart on the East and West Coasts. Considering all of the variables involved with each set of Zt measurements, the closeness of the data demonstrated a high confidence level in the accuracy of the a.c. Zt measurements.

In addition to the measured data, the program required that an EMI model be developed to predict the performance of the new technology SGA. If measured and predicted data were reasonably close (within 10 dB) then confidence in the measured performance would be very high. Also, and perhaps most important, the model would allow potential SGA improvements to be evaluated on the computer, thereby saving time and money normally expended by conducting SGA performance testing. The mathematical SGA EMI model developed by Dr. Ralph Showers and Mr. Steve Peters [5] also falls within 4 dB of the NUSC and G & H test data illustrated in figure 4. The model data and the measured data is for an early version of the new technology SGA. This SGA had a fingered shield contactor rather than the solid contactor ultimately used to optimize SGA performance.

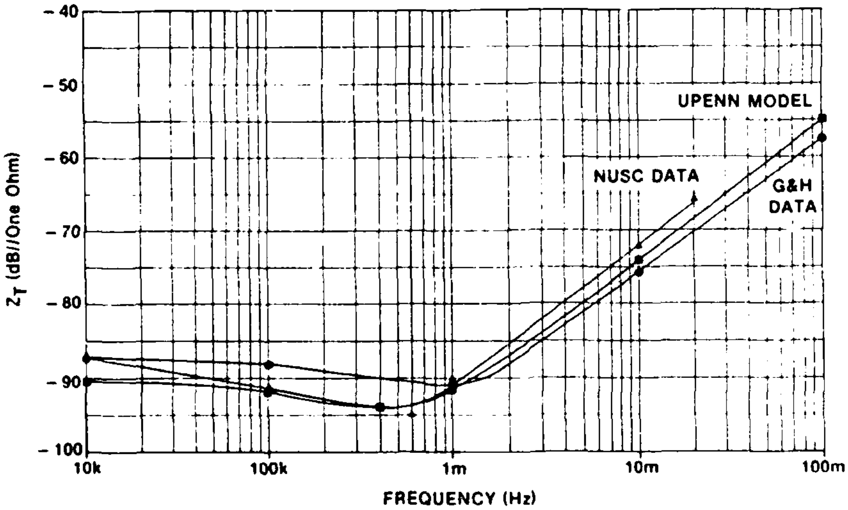

Figure 4: Comparison of NUSC (Shielded Room) and G&H (Triaxial Fixture) Measurement Systems Test Data With the UPENN EMI Model

EVALUATION OF THE D.C. PERFORMANCE OF EXISTING AND NEW TECHNOLOGY SGAs

D.C. TEST CONFIGURATIONS

It was demonstrated in the EMC laboratory at NUSC/NL that a.c. values of Zt were too small to be measured in the shipboard environment due to other nearby hull penetrations that caused EMI coupling between topside and below-deck areas. This coupling necessitated that all a.c. SGA performance measurements be made in the laboratory. However, it was possible to make shipboard measurements of d.c. Zt. Even in the electromagnetically noisy shipboard environment, whenever a large d.c. current, I(in), was injected on the input side of the cable shield, a voltage, V(out), could be measured on the SGA output side of the cable shield. This measurement was necessary to verify the initial and periodic integrity of the shield to ground contact. As shown in figure 5, d.c. resistance measurements were made between test points A through E by driving 4 amperes of d.c. current down the cable shield and measuring the d.c. voltage between test points A through E. The physical differences between the two SGAs installed on the ship and the exact location of each test point is illustrated in figure 6.

NEED FOR KICKPIPE EXTENSION

The SGAs are designed to screw into a standard kickpipe (an environmentally sealed cable penetration through the deck) that is welded to the deck, and a method was needed to measure the electrical performance of the SGA-to-kickpipe thread interface. To accomplish this goal, a kickpipe extension was made from the same aluminum alloy as the kickpipe. The interface between the SGAs and the extensions had the same electrical, mechanical, and electro-chemical properties that the SGA-to-kickpipe interface would have had. Using the extension allowed removal of the SGA-to-kickpipe extension interface from the ship without disturbing the cable shield-to-SGA connection integrity, thereby permitting a repeat of the pre-environmental EMI testing in the electromagnetically quiet laboratory environments of NUSC and G & H.

D.C. PERFORMANCE AFTER FIVE MONTHS OF SHIPBOARD EXPOSURE

Measurements of voltage between test points A & D (see figure 5) for both an existing spring compression style SGA and a first generation fingered shield contactor SGA, indicated the following:

1. Initial pre-installation d.c. values of Zt for both devices were very similar,

2. After five months of exposure to the shipboard environment:

   a. the d.c. Zt for the 1st generation smart-soldered style SGA increased (degraded) by 2.1 dB, (3.7 to 4.7 mV)/4A.

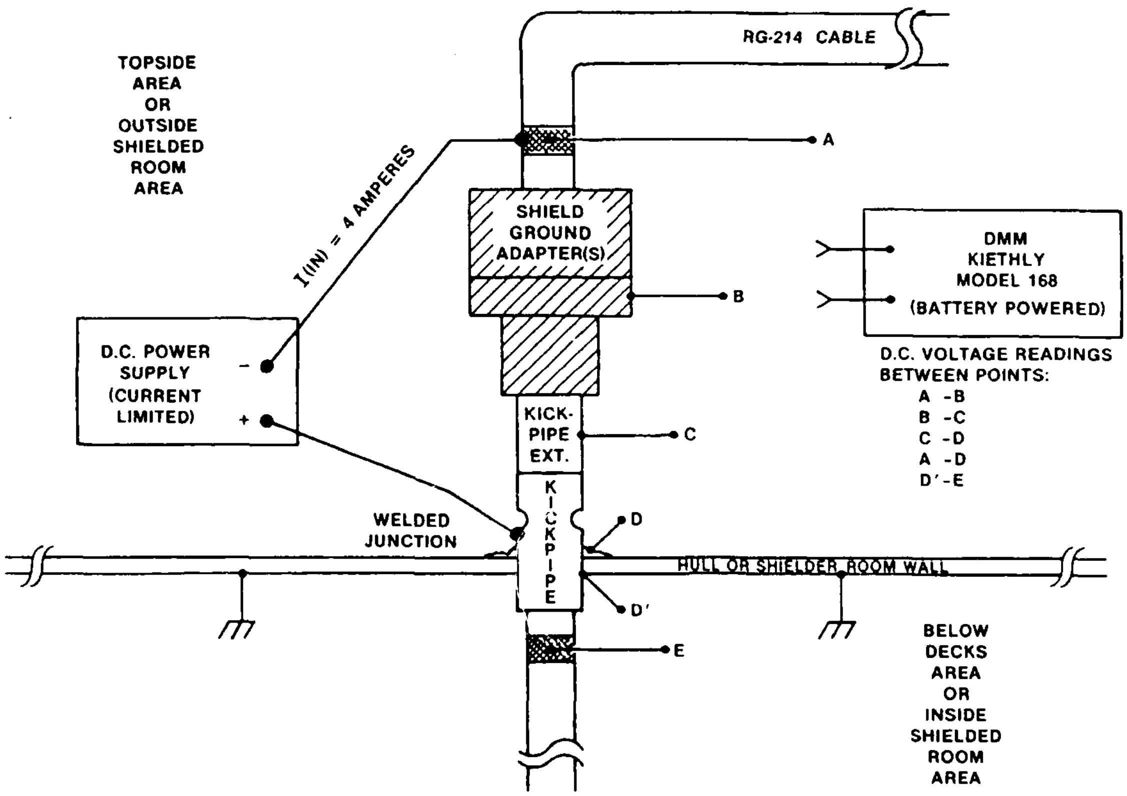

Figure 5: D.C. Transfer Impedance Measurement Configuration (Shipboard Measurement)

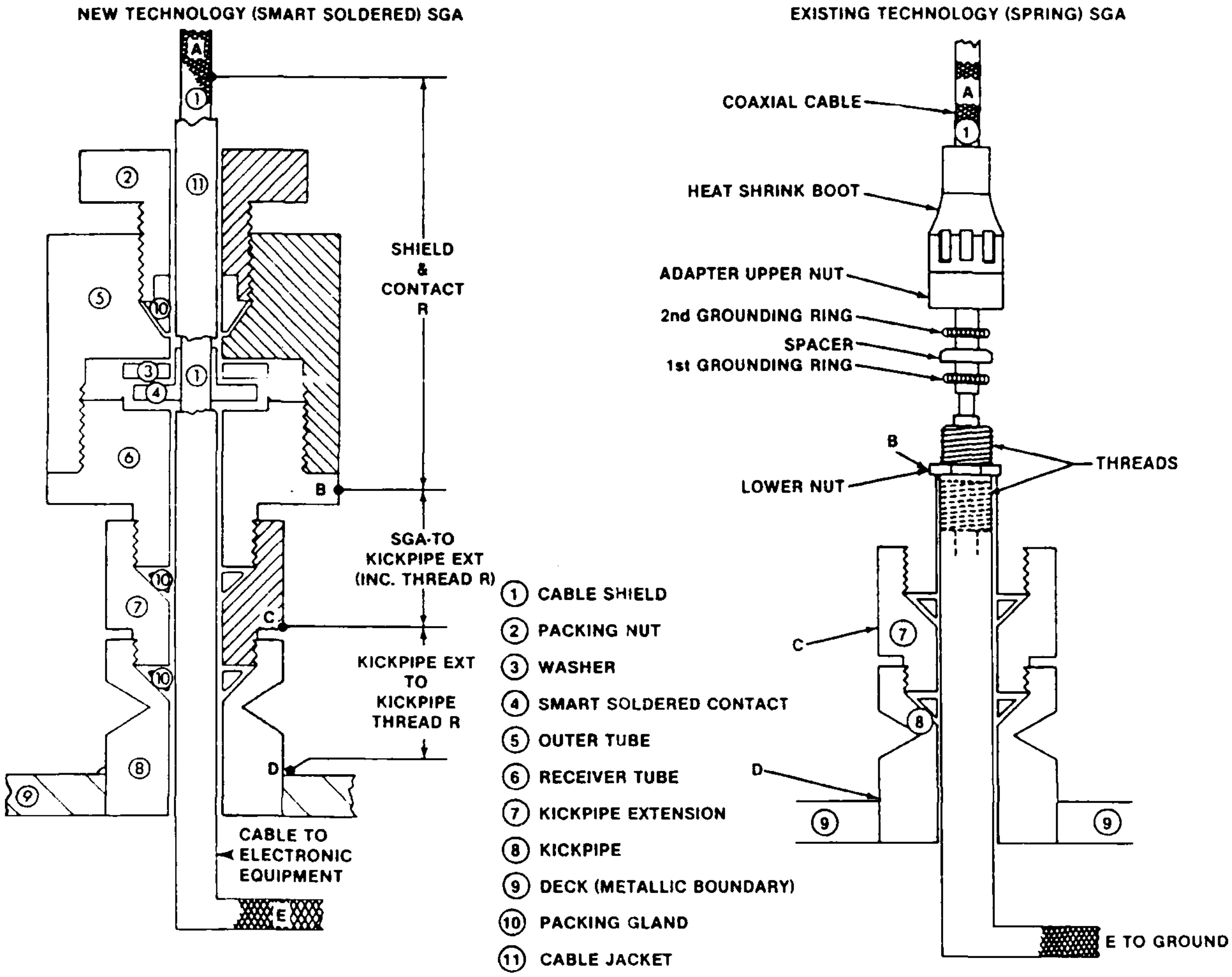

Figure 6: Physical Models of the New Technology (Smart Soldered) and Existing Technology (spring-compression) Shield Ground Adapters

b. the d.c. Zt for the spring compression style SGA increased (degraded) by 17.1 dB, (5.4 to 38.8 mV)/4A.

3. Even at that early time, preliminary analysis indicated that threaded interfaces, such as the SGA-to-kickpipe extension interface, might be very crucial in determining long term SGA performance.

LONG TERM PERFORMANCE VALIDATION OF EXISTING AND NEW TECHNOLOGY SGAs

EVALUATIONS OF SGAs AFTER ONE YEAR OF SHIPBOARD EXPOSURE

Utilization of the kickpipe extension discussed above was to have permitted the removal of the SGAs from the ship without disturbing the cable shield-to-SGA connection, thereby permitting a repeat of the pre-installation a.c. EMI testing that had been conducted in the quiet laboratory environments. Inconsistent post-installation laboratory a.c. and d.c. Zt values indicate that this goal may not have been achieved i.e., apparently, movement of the SGAs during removal from the ship, during testing at NUSC, or during shipment to the West Coast for G & H testing caused physical stress/vibration within the SGA that resulted in inconsistent Zt data.

SHIPBOARD MEASUREMENTS: D.C. PERFORMANCE-VS-TIME

The d.c. measurements conducted on the ship were a good barometer of SGA performance over time. As shown by other laboratory measurements, the low frequency a.c. and the d.c. data points are almost exact. In fact, it was this difference in d.c. data points (d.c. ship & d.c. lab & a.c. lab) that alerted the measurement team that movement of the SGA was causing changes in the SGA's performance.

Figure 6 illustrates the d.c. performance degradation-vs-time of the existing (spring) technology SGA over the 12 month period of time it was installed on the ship. The d.c. measurement results plotted in figures 7 & 8 were measured at the

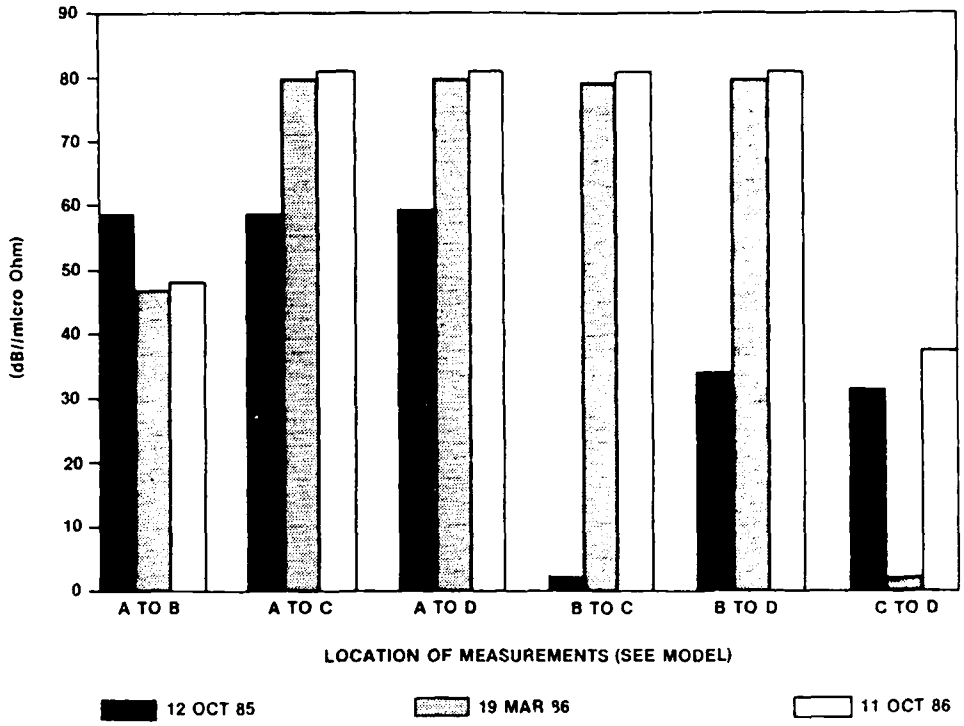

Figure 7: Shipboard D.C. Measurements-vs-Time for the Existing (Spring-Compression) Technology SGA

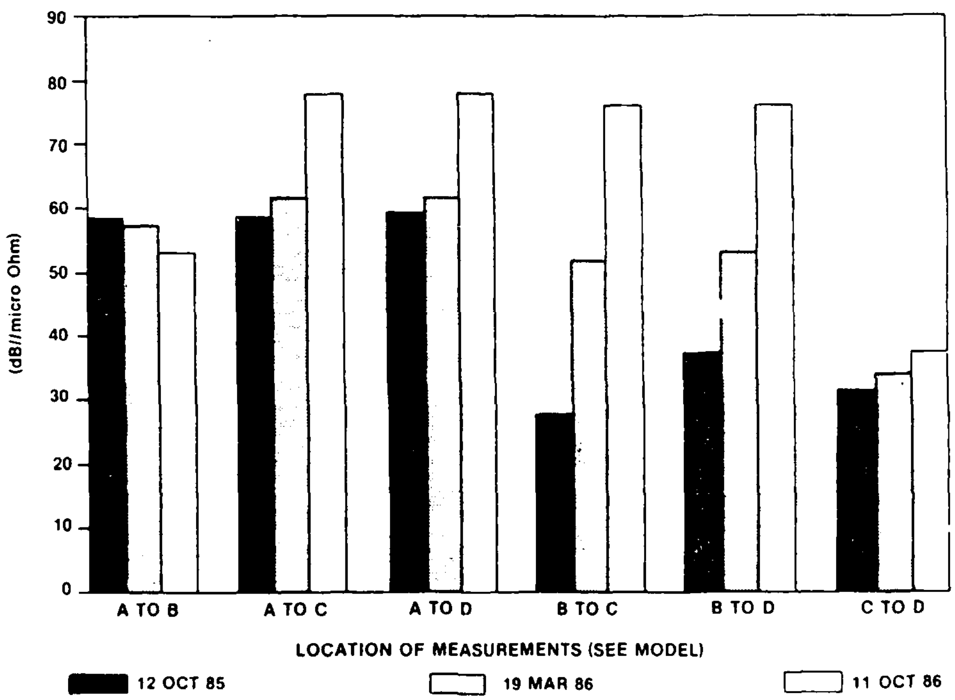

Figure 8: Shipboard D.C. Measurements-vs-Time for the New (Smart-Soldered) Technology SGA

points illustrated in figure 6. Measurement point A-to-B includes the cable shield and grounding ring(s) or fingered shield contactor to SGA body resistance. Measurement point B-to-C includes the SGA-to-Kickpipe Extension resistance and the resistance associated with the first set of threads. These areas of the SGA are the most significant when considering the SGA's long term performance.

The following observations, taken from the data in figure 7, summarize the long term d.c. performance of the existing (spring) technology SGA:

a. the d.c. performance of the cable shield and the spring contact portion of the SGA (A-B) actually improved with time (875/225/255 micro-Ohms),

b. the d.c. performance of the 1st thread interface (B-C) suffered tremendous degradation with time (1.3/9, 300/11, 100 micro-Ohms),

c. the d.c. performance of the 2nd thread interface (C-D) caused initial degradation (50 micro-Ohms), but it was quickly masked by the high degradation of the first thread interface,

d. the d.c. performance of the total SGA (A-D) was dominated by the degradation at the thread interfaces, particularly the 1st thread interface. SGA performance degraded from 950 to 9,800 to 11,400 micro-Ohms.

The following observations, taken from the data in figure 8, summarize the long term d.c. performance of new smart-soldered technology SGA:

a. the d.c. performance of the cable shield and the smart soldered contact portion of the SGA (A-B) improved slightly with time (863/750/463 micro-Ohms),

b. the d.c. performance of the 1st thread interface (B-C) suffered significant degradation with time (25/400/6600 micro-Ohms),

c. the d.c. performance of the 2nd thread interface (C-D) was 37.5 micro-Ohms (initially) and a low 7.5 micro-Ohms (finally),

d. the d.c. performance of the total SGA (A-D) was dominated by the degradation of the thread interfaces, particularly the 1st thread interface. SGA performance degraded from 938 to 1200 to 8100 micro-Ohms.

LONG TERM A.C. PERFORMANCE EVALUATION OF EXISTING & NEW TECHNOLOGY SGAs

As discussed earlier, the a.c. performance of the SGAs could only be evaluated in the laboratory. The kickpipe extensions were fabricated to assist in the removal of the SGAs without affecting their grounding performance.

EXISTING TECHNOLOGY SGA A.C. PERFORMANCE TEST RESULTS

Pre and post installation a.c. performance testing was accomplished using the NUSC test procedure. The results of this testing, conducted 6 hours, 24 hours, and 12 months apart, are shown in figure 9. The range in the short term (hours) test results was discussed at the last IEEE EMC Symposium [2]. Although a function of frequency, the range in

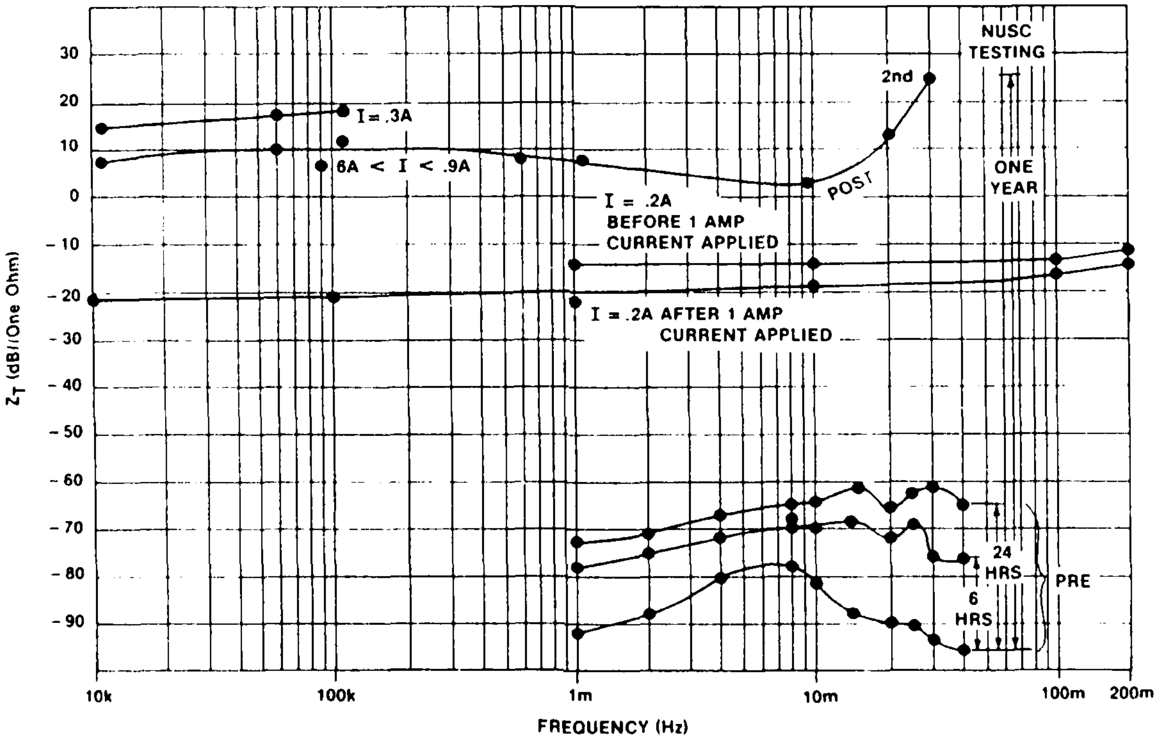

Figure 9: Existing Technology, New Construction SGA A.C. Transfer Impedance: Pre & Post Installation NUSC and G&C Test Data

performance nominally ranged from -96 to +24 dB//one-Ohm. This represents a 120 dB range in performance-vs-time. It should also be noted that the performance of the device was dependent on the amount of current driven down the cable shield and the SGA. A 6 to 10 dB increase in the current brought about a 6 to 9 dB increase in the SGA's performance.

G & H also conducted post installation testing on the existing technology SGA. This testing was conducted after the NUSC testing and the test results on the SGA seem to indicate that the SGA may have been physically stressed during shipment and/or testing. The G & H testing shows significantly better test results, ranging from -20 to -30 dB//one-Ohm better than the NUSC testing on the same SGA. We also see that the SGA performance once again varies due to the amount of current driven down the cable shield and SGA. After increasing the current by 14 dB and then retesting with the original current value of .2 amps, the performance improved by approximately 6 dB.

Evaluation of the a.c. performance for the existing technology SGA shows a significant amount of variation between both NUSC pre and post installation test data as well as the G & H post installation test data. This may have been caused by mechanical vibration/stress of the test sample between removal from the ship and between East and West Coast testing. This would tend to suggest that either the kickpipe extension did not work as planned or this SGA's performance is highly dependent on contact resistances/impedances. Hoeft has indicated [7] that "contact impedance is the major electromagnetic hardness degradation factor in cables, connectors, and cableways." It would appear that kickpipe thread areas would have to be added to Mr. Hoeft's list of components having high degradation factors. It was verified earlier in this paper (see figure 4) that a.c. performance testing on the same SGA yielded results within 4 dB of each other when NUSC and G & H test methods were compared. This fact, in addition to the high degree of correlation to the SGA EMI model developed by Showers [5 & 6], suggests that the measured variation was indeed caused by this type of SGA rather than by the test procedures.

NEW TECHNOLOGY SGA A.C. PERFORMANCE TEST RESULTS

Pre and post installation a.c. performance testing was accomplished using the NUSC test procedure. The results of this testing, conducted 12 months apart, are shown in figure 10. There was no change in performance during the first 24 hrs. The range in the preinstallation a.c. performance was from -85 to -65 dB//one-Ohm. The post installation testing ranged from -55 to -40 dB//one-Ohm. The difference between the curves in figure 10 illustrates a 20 to 30 dB degradation over the one year period of time it was installed on the ship.

G & H also conducted post installation testing on the same new technology SGA. Over a frequency range from 10 kHz to 200 MHz, this testing resulted in SGA performance ranging from -43 to -31 dB//one-Ohm.

Variation in a.c. performance for this SGA indicate significantly less variation between both pre and post installation testing and between NUSC and G & H test data. Therefore, this type of SGA appears to be less susceptible to movement in the cable-SGA-kickpipe assembly.

IMPROVED SOLID CABLE SHIELD CONTACTOR: NEW TECHNOLOGY SGA DEVELOPED

As the existing and the new technology SGAs were environmentally aging on the test platform, an improved new technology SGA was developed. This improved version utilized a new (RG) cable shield contactor that was almost solid as compared to the earlier version that was fingered. Both EMI model and EMI test data indicated that the fingered version caused decreased performance at higher frequencies. Figure 11 illustrates a range of SGA transfer

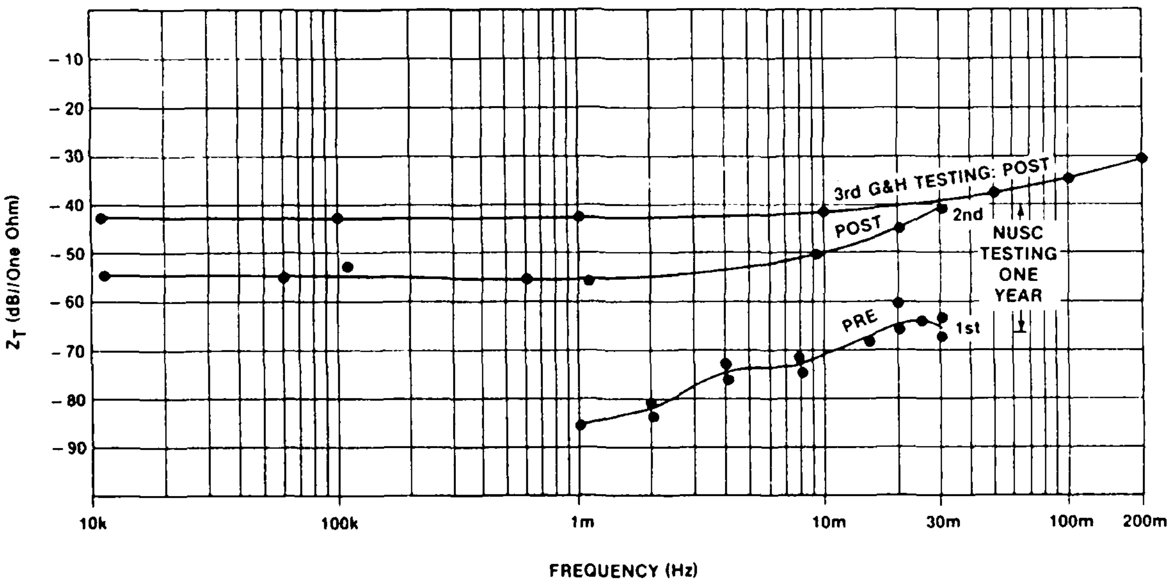

Figure 10: New Technology New-Construction SGA A.C. Transfer Impedance: Pre & Post Installation NUSC and G&H Test Data

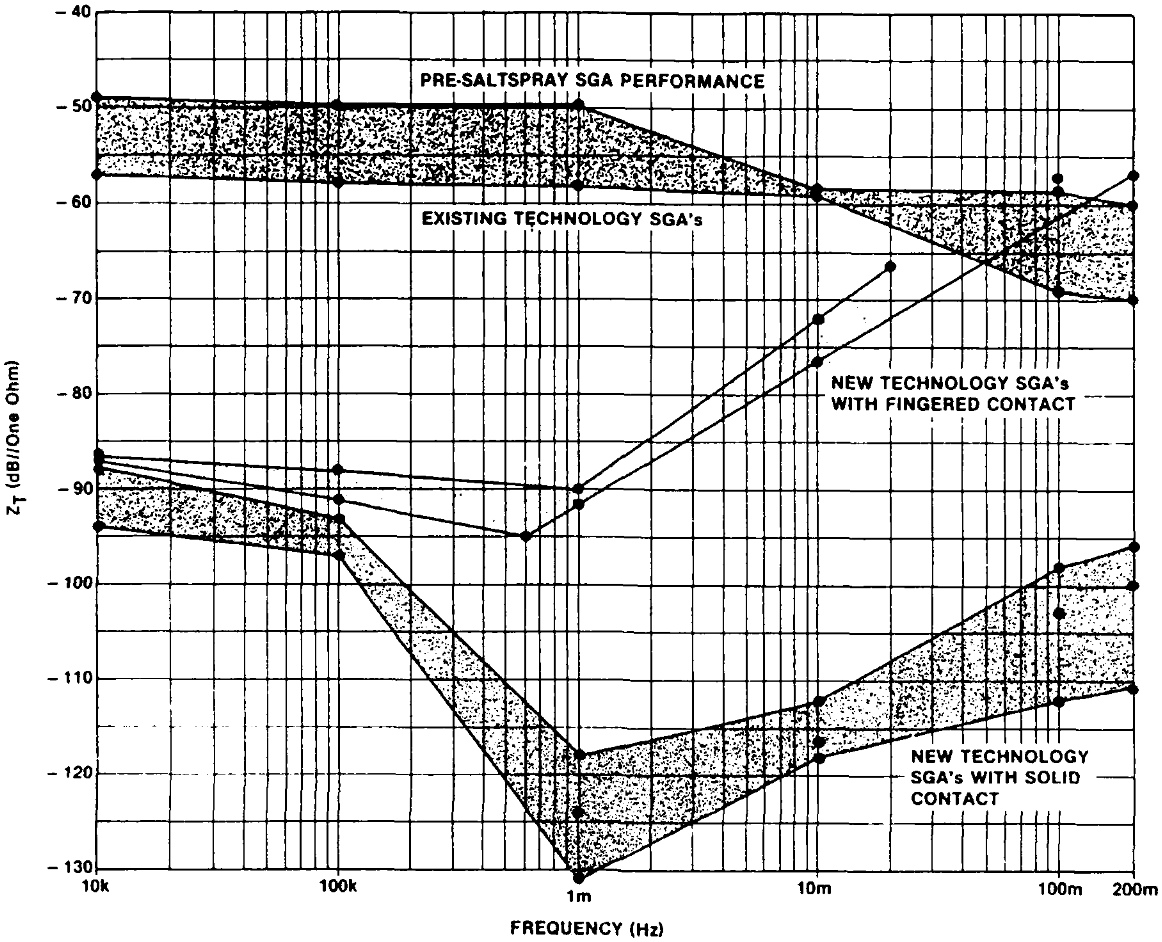

Figure 11: Comparison of Transfer Impedance Test Data For Three Types of RG-214 Style SGA's

impedance (Zt) test data initially measured on the existing technology SGA (top curves), the new technology SGA (middle curves), and the new technology SGA with the improved cable shield contactor (lower curves). Even with a range of SGA samples tested, it can be seen that the new solid shield contactor dramatically improves the high frequency performance of the SGA.

CONCLUSIONS

a. The d.c. performance of the cable shield contact area improved slightly with time for both styles of SGAs,

b. the long term d.c. performance of the SGAs was completely dominated by the resistance of the thread interfaces required to connect the SGAs to the ship's hull,

c. the spring contact SGA's short-term a.c. performance could be significantly changed by "re-torqueing" it,

d. the performance of the spring technology SGA showed a variation in performance directly related to the amount of current flowing on the cable's shield (a current increase of 10 dB (NUSC) or 14 dB (G & H) improved performance by 9 or 10 dB, respectively),

e. as measured by the NUSC testing, the degradation in performance in the spring contact SGA over time was much worse than the new technology SGA over time (120 dB-vs-44 dB) (+24 to -96 dB) & (-85 dB to -41 dB),

f. thread resistance/impedance is a dominant form of degradation not actually within the SGA but one that occurs at the SGA-to-kickpipe interface,

g. the d.c. and a.c. performance testing of the new technology SGA occurred on an early device that utilized a "fingered" cable shield-to-SGA contactor; subsequent EMI modelling and testing has indicated that a significant performance improvement (up to 35 dB) can be obtained at higher frequencies when utilizing a "solid" cable shield contactor, and

h. it is necessary to consider the life cycle performance of d.c. and a.c. EMI grounds.

RECOMMENDATIONS

1. Develop an EMI model to describe the degradation caused by the kickpipe threads; this would have

application for a wide range of EMI grounding devices,

2. Develop an electrochemically compatible solution to the thread degradation problem and evaluate its long term success by shipboard installation and/or accelerated life cycle testing,

3. Develop a military performance specification for the solid cable shield contactor new technology SGA to permit it to be used on a retrofit basis on Naval platforms,

4. Install a new technology SGA, with the solid shield contactor, on a test platform in conjunction with a thread "fix" to ensure that the highest long-term SGA performance is achieved to reduce below-decks electromagnetic (EM) levels caused by EM currents.

ACKNOWLEDGMENTS

Support for this project was provided by the Office of The Chief of Naval Research/Office of Naval Technology; Submarine Technology Program Element; Program Element Manager is Mr. Gene Remmers, Code 233. Block Program Manager for the Submarine Technology Block Program is Mr. Lincoln Cathers, Code 012.4, of the David Taylor Naval Ship Research & Development Center. Principal Investigator of "The Ships Below-Decks EMC Program" is Mr. David S. Dixon, of the Naval Underwater Systems Center, Code 3431. Triaxial fixture test method and measurement data was provided by Mr. John Miller, consultant.

REFERENCES

1. MIL-STD-1310(E), "Shipboard Bonding, Grounding and Other Techniques for EMC and Safety."

2. David S Dixon & Stanley Sherman, "Reduction of EMI/EMP Shield Currents Using An Improved Shield Ground Adapter," 1986 IEEE International Symposium On EMC, September 1986.

3. H. Kent. "Self Heating/Self Soldering Make-Break Connectors." Electronic Connector Study Group, 18 Nov 1985.

4. M. Van Brunt, "Advanced Current Shunting Device for Shielded Cable and Conduit," 1986 IEEE International Symposium On EMC, September 1986.

5. R.M. Showers and S. Peters, "Development of Models for the Shield Ground Adapter," UPENN RPT MSEE-F-85-3, 31 Dec 1985.

6. R.M. Showers, "Development of a Model for the Shield Ground Adapter," Proceeding of the 1987 IEEE International Symposium on EMC, August 1987.

7. L. O Hoeft, "The Case for Identifying Contact Impedance as the Major Electromagnetic Hardness Degradation Factor," 1986 IEEE International Symposium on EMC, September 1986.

APPENDIX B

DEVELOPMENT OF A FULL PERFORMANCE COMPOSITE CONNECTOR WITH LONG TERM EMI SHIELDING PROPERTIES

DEVELOPMENT OF A FULL PERFORMANCE COMPOSITE CONNECTOR WITH LONG-TERM EMI SHIELDING PROPERTIES

by

James V. Masi, Member IEEE
Department of Electrical Engineering
Western New England College, Springfield, MA, USA

David S. Dixon, Member IEEE
Naval Underwater Systems Center, New London, CT, USA

Maurice Avoux
formerly of G & H Technology, Inc., Camarillo, CA, USA

ABSTRACT

The purpose of this paper is to discuss two phases of the effort required to develop a full MIL-SPEC connector made from composite materials composed of conducting particles, fibers, or flakes in a matrix of polymeric material. This connector is designed to satisfy a full range of electromagnetic, chemical, and mechanical properties, including corrosion resistance to hostile environments and electrochemical compatibility with electronic cabinets made from aluminum.

The first part of this paper will discuss the factors involved in the composite material/filler selection process, including existing and proposed materials/fillers. The second part will discuss the development of a mathematical model which gives the basis for prediction of some of the electromagnetic properties of a composite material.

Suggestions for further work on materials and modeling are given, with special reference to emerging techniques and materials.

BACKGROUND

Given the crowded electromagnetic environment as well as the potentially hostile land and marine environments existing today, there are many incentives to develop a connector, made from composite polymeric materials, that will have good and non-degrading EMI performance over time. To be useful for a range of applications, the connector must be: resistant to chemical attack, immune to shock (both thermal and mechanical), corrosion resistant when connected to aluminum structures, lightweight, machinable, moldable, capable of operation in high temperature environments (> 200° C), and provide better EMI shielding effectiveness (over time) than existing composite technologies. Such were the goals established for the EMI development program.

A cursory evaluation of several ongoing material development efforts indicated that the key to reaching these goals was to assemble a proper mix of technologists who would be capable of developing a full MIL-SPEC connector with performance approaching that of existing metallic connectors. A development team was therefore formed that contained the following expertise:

a. theoretical electromagnetic interference (EMI) personnel,

b. theoretical materials personnel,

c. EMI test personnel, and

d. connector manufacturing and test personnel.

It was believed that this mix of technologists, all things being equal, would have the highest probability of developing a composite connector with all the desired qualities.

INITIAL RESIN/FILLER SELECTION AND EVALUATION

The high temperature thermoset and thermoplastic resins listed in Table 1 were initially selected for evaluation due to their working temperature, strength, deflection temperature, chemical resistance, and toughness.

	RESIN	TEMPERATURE
1.	POLYETHERETHERKETONE (PEEK)	282° C
2.	POLYPHENYLENE SULFIDE (PPS OR RYTON)	232° C
3.	POLYAMIDEIMIDE (PAI)	220° C
4.	POLYIMIDE (PI)	204° C
5.	POLYETHERSULFONE (PES)	180° C
6.	POLYARYLSULFONE (PAS)	180° C
7.	POLYETHERIMIDE (PEI)	180° C
8.	LIQUID CRYSTAL POLYMER (LCP)	240° C

TABLE 1: POTENTIAL HIGH TEMPERATURE THERMOSETS & THERMOPLASTICS MIL-C-38999, Series IV; MIL-C-28840.

Initially, due to their good electrical conductivity and expected good shielding properties, various combinations and percentages of aluminum flake and fiber were compounded with the above resins. The products were tested and indicated that most of the aluminum/resin combinations suffered from electrical conductivity degradation and significant weaknesses in the injected molded materials. Close investigation indicated that the aluminum filler oxidized very rapidly, especially during temperature cycling, thereby causing a loss in the composite's electrical conductivity, with subsequent loss in both material shielding properties and mechanical properties. Electrical conductivity degraded typically over three orders of magnitude, while mechanical properties had typical degradations of over 30%. This effect is not clearly noted in literature describing the subject[1].

This forced the program into a reevaluation period, in order to discover a metallic or semi-metallic filler or combination of fillers that would not degrade the inherent resin strength and would provide a reasonable amount of electromagnetic shielding that would not degrade with time or temperature. Several promising resin/filler combinations that appear to meet the requirements discussed above have now been compounded. Graphite and nickel coated graphite fibers in these resins were to be used as comparisons for conductivity, corrosion, and modeling, but were not considered to be viable, due to their causal role in the corrosion of aluminum parts in contact with these composites [2].

Resins that were retained for further study include polyimide (PI), polyetheretherketone (PEEK), and polyetherimide (PEI). These resins have good moldability, good to excellent machinability, and have continuous use temperatures exceeding 200°C (loaded). Color was not deemed a determining factor in resin or filler selection.

Fillers presently being evaluated include PAN graphite fibers and flake, nickel coated graphite fibers, carbon particles, indium/tin oxide (ITO) particles, ITO particles with graphite fibers, and aluminum coated E-glass. Early in the study, aluminum coated E-glass proved to be an improper choice due to the chemical tendency of the aluminum to scavenge the oxygen from the underlying glass, causing the aluminum to oxidize and become an insulator rather than a conductor. Mechanical properties were observed to degrade rapidly, causing pullaway of fiber from resin.

The galvanic properties of metals and alloys are given in Table 2 below. The table shows the increasing tendency of the material to corrode as it becomes more anodic.

< — — — — — — — — MORE ANODIC

GROUP I	GROUP II
MAGNESIUM	ALUMINUM
MAGNESUIM ALLOY	ALUMINUM ALLOY
ALUMINUM	BERYLLIUM
ALUMINUM ALLOY	ZINC
BERYLLIUM	CHROMIUM
ZINC	CADMIUM
CHROMIUM	CARBON STEEL

MORE CATHODIC — — — — — — — — <

GROUP III	GROUP IV
CADMIUM	BRASS
CARBON STEEL	STAINLESS STEEL
IRON	COPPER & ALLOYS
NICKEL	NICKEL/COPPER
TIN	ITO
TIN/LEAD	MONEL
LEAD	SILVER
BRASS	GRAPHITE
STAINLESS STEEL	RHODIUM
COPPER & ALLOYS	PALLADIUM
NICKEL/COPPER	TITANIUM
MONEL	PLATINUM
ITO	GOLD

TABLE 2: GROUPING OF MATERIALS BY ELECTROCHEMICAL COMPATIBILITY

The unique properties of certain oxides and catalytic-behaving materials to "self-adjust" their electrochemical EMF's (either by oxygen manipulation or other charge transfer) make them extremely attractive in minimizing corrosion due to the dissimilar galvanic potentials. In addition, some of these oxides are semiconductive, allowing for overall improvement of shielding effectiveness (S.E.) when the materials are fabricated into a connector that must be attached to an electronic enclosure. It is also expected that the S.E. of these materials will improve with applied voltage/current, thereby making them perform better during high level electromagnetic field exposure.

Presently, tests are being made on all of the above composite resin/filler variations. Electrochemical tests are being made to verify the expected behavior of these materials when galvanically coupled to aluminum components. EMI shielding, as well as basic complex impedance calculations and tests are being performed to verify models postulated upon distributed parameter calculations. Early results are encouraging and not without the expected undesirable materials interactions between resins and filters.

The properties of a composite depend on a wide variety of component properties. Among these are relative proportions of resin and filler, size, shape, state of agregation or agglomeration, relative dispersion, and orientation of filler. Finally, the level of interphase adhesion affects ultimate strength and elongation and is a measure of the unwanted condition of "pullaway". For example, for fibers with circular or square cross-section, one of the simplified methods of predicting the composite modulus, tensile or transverse, (the Halpin-Tsai *equation*) is:

(1) Tensile: $E_c = V_f E_f + V_m E_m$, and

(2) Transverse: $E_c = [(1 + 2\eta V_f)/(1 - \eta V_f)]E_m$,

where

$\eta = \{[(E_f/E_m)-1]/[(E_f/E_m)+2]\}$,

E_c is the modulus of the composite, E_f and E_m are the moduli of the filler and the matrix, respectively, and V_f and V_m are the volume fractions of the filler and matrix, respectively. These are the approximate bases on which the mechanical properties of the ideal composite were pre-estimated.

A THEORETICAL MODEL TO PREDICT THE ELECTROMAGNETIC PROPERTIES OF COMPOSITE MATERIALS

There are a number of theoretical models which conditionally predict the electrical properties of composites based upon a hopping model[3], percolation theory[4], critical loading[5], and simple RC networks[6]. A baseline effort has been made to establish, not only a verifiable model, but one which established the electromagnetic properties of the composite when given a set of specific component material parameters. As a result of the effort, an interactive computer program was written and is evolving, as the model and data dictate, into a tool which will allow for user input of component (fiber and filler) parameters found to be of electromagnetic importance. This program calculates properties from d.c. to one gigahertz, and gives output which can be verified by testing specimens, either in a flanged coaxial holder for shielding effectiveness measurements (Figure 1), in an admittance bridge (Figure 2), or in a network analyzer (Figure 3).

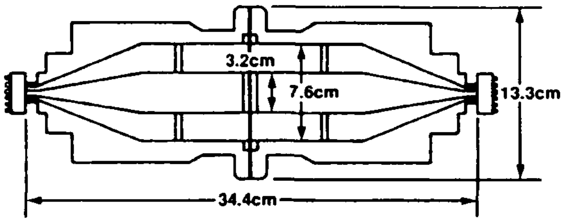

FIGURE 1: FLANGED COAXIAL HOLDER

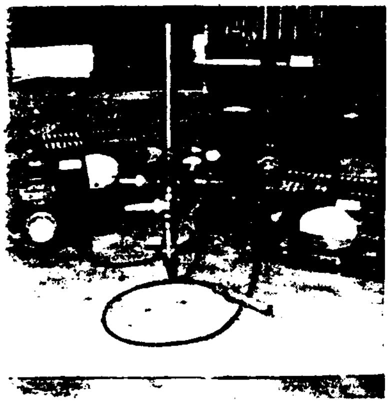

FIGURE 2: ADMITTANCE BRIDGE

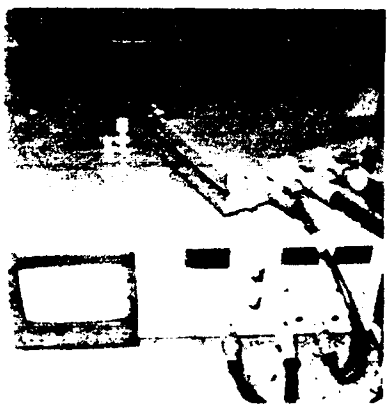

FIGURE 3: NETWORK ANALYZER

The model shows that polymeric composite slabs containing conductive particles, flakes, fibers, or combinations of these, have measurable transmission, reflection, and absorption coefficients. The filler morphology varies characteristics for electromagnetic scattering and absorption in the composite materials. Theoretical results for optimum design of EMI shielding could be derived by using statistical field theory or by distributed parameter network modeling using frequency and field dependent components in the analysis. The model should also be applicable to the construction of radio anechoic chambers and electronic packaging. Two approaches were merged into one to analyze this problem. The stochastic field theory results were superimposed on a conventional three-dimensional impedance model with frequency and field dependent terms [7], [8], [9].

Three factors are prime in the determination of the behavior and properties of composites, both from a mechanical and electrical point of view, exclusive of the approach:

1. The fundamental materials of which the composite is composed;
2. the morphology and structural disposition of the constituents; and
3. The multifactorial interaction among the constituents (e.g. chemical, mechanical, and electrical).

Using the filler model which relates the resistivity of the filler material to that of the composite via the volume fraction of the filler, the d.c. resistivity of the combination can be calculated.

$$(3) \qquad \rho + (V_f/3)\,[1/(1-\sqrt{V_f}/3)]\,\rho_o.$$

Using form factors for the particle, flake, or fiber, and combining this with a three-dimensional matrix, leads to a solvable set of equations involving resistors, capacitors, and inductors at various frequencies and fields. The model needs inputs with respect to electric field and frequency dependence of the resistive and reactive elements, i.e. $R(E,\omega)$ and $X(E,\omega)$. Typical materials are being tested for d.c. and high frequency properties in order to "fit" the functional dependence of $R(E,\omega)$ and $C(E,\omega)$. First iterations are in progress with more sophisticated measurements and model refinements to follow. This extended circuit approach will be later compared with more complex statistical field theory approaches now in progress. It is expected that, at least, a model will be proposed which can serve as a "first test" for new electrical composite formulations.

D.C. CASE

A composite sample under an applied d.c. field has its potential distribution curves bent more drastically over the conducting filler contacts due to space charge. The equivalent circuit representation is shown in Figure 4. Within at least a half order of magnitude, the impedance for a three dimensional array of these components is approximately the value of Z for the simple network. Ignoring, for the time being, distributed parameter considerations, the time constant of such a circuit at a given electric field strength, E, is

$$(4) \qquad T = R_o[R(E)C(E)]/[R(E) + R_o] \, ,$$

assuming smooth contours on the particle/flake/fiber and an electrically homogenous, isotropic polymer matrix.

A number of researchers have noted that current controlled negative resistance (C.C.N.R.) is observed (voltage dependent threshold initiation)[10]. Local heating of the matrix/conductive filler is deemed to be the cause, the result being quasi-filimentary conduction. This implies that, as the voltage (field) increases across a composite element, its conductivity and, as a result its shielding effectiveness, increases. This effect is enhanced by certain fillers which themselves exhibit C.C.N.R. or voltage controlled negative resistance (V.C.N.R.).

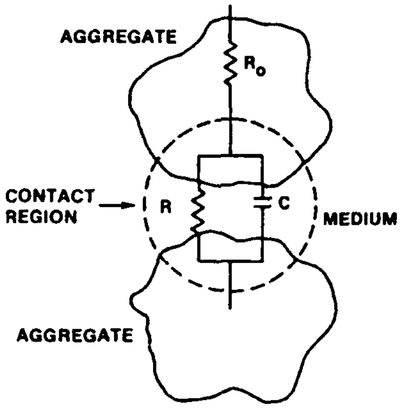

FIGURE 4: EQUIVALENT CIRCUIT

A.C. CASE

Ideally, one would like to see a medium with just the right combination of coarse and fine[11] particles to provide for maximum composite conductivity and maximum mechanical strength, as shown in Figure 5. According to the electrical model shown (ignoring for now the aforementioned inductive component), the equivalent $R_0/R(E,\omega)/C(E,\omega)$ circuit impedance should decrease with increasing frequency. This combined with C.C.N.R. or V.C.N.R. makes the composite with semiconducting particles, flakes, or fibers (or combinations thereof) an improved shield, not only for EMI, but also for electromagnetic pulse (EMP) applications.

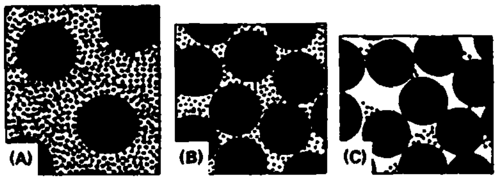

(A) excess of fine particles; (B) optimum composition; (C) excess of coarse particles.

FIGURE 5: PACKING OF FINE AND COARSE PARTICLES

Applying the effective medium theory[12] to the conductivity and the complex dielectric constant of the composite material, one can obtain a relationship between the properties of the matrix and those of its components by

$$(5) \qquad V_f(\varepsilon_f^* - \varepsilon_c^*)/(\varepsilon_f + 2\varepsilon_c^*) = -(1-V_f)(\varepsilon_m^* - \varepsilon_c^*)/(\varepsilon_m^* + 2\varepsilon_c^*) ,$$

where

ε_f^*, ε_m^*, and ε_c^*

are the complex dielectric constants of the filler, matrix, and composite, respectively, and V_f is the volume fraction of the filler.

In general,

$$(6) \qquad \varepsilon^* = \varepsilon_r - j\sigma/\varepsilon_0\omega ,$$

where σ is the conductivity in mhos/m, ε_0 is the permittivity of free space (approximately 8.85×10^{-12} F/m, ω is the angular frequency in radians/seconds and ε is the real, relative dielectric constant. So, the equivalent circuit now becomes a matter of defining a loss tangent of the medium, the dielectric constant of the medium, the conductivity of the flake/fiber/particle, the complex dielectric constant of the filler, the effective morphology of the filler, and the fraction of filler participating in the process. The shape function of the filler is obviously important in the estimation.

RESULTS

Using the form factors for the particle, flake, or fiber involving cross-sectional area considerations of the filler (A), inter-fiber/flake/particle spacing (d), frequency ε, resistivity (ρ) as in equation (3), the impedance of the specimen can be expressed by

$$(7) \qquad Z = -j/[\rho(\varepsilon_0\varepsilon_r A/d) - j(A/\rho_p d)] + R_0 .$$

The program written to implement this effort is simple and interactive. The results were compared initially with graphite PAN fiber samples in polycarbonate and carbon particles in polycarbonate. Measurements of impedance-vs-frequency, for 40 weight percent fiber cylindrical samples are shown in Figure 6. Measurements on the rectangular samples are shown in Figure 7. Table 3 depicts calculated-vs-measured values for impedance and phase angle for cylindrical and rectangular samples of the short fiber variety.

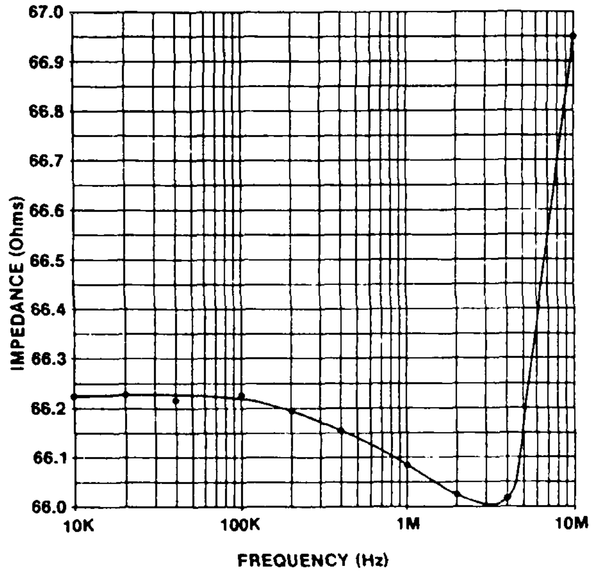

FIGURE 6: MEASURED IMPEDANCE-VS-FREQUENCY FOR CYLINDRICAL SAMPLE OF GRAPHITE IN POLYCARBONATE (@.1V)

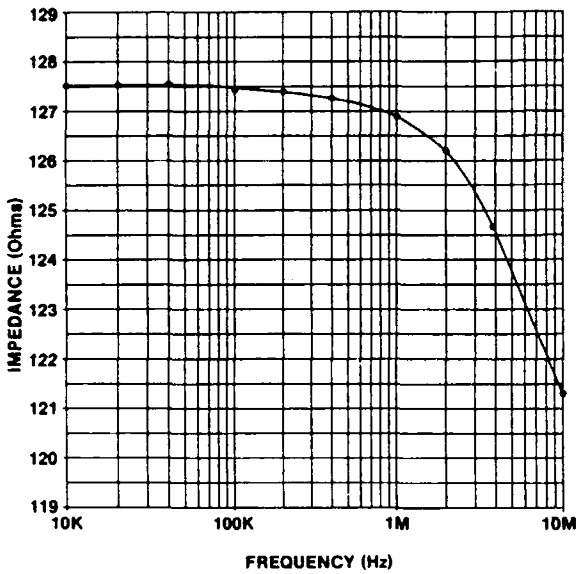

FIGURE 7: MEASURED IMPEDANCE-VS-FREQUENCY FOR RECTANGULAR SAMPLE OF GRAPHITE IN POLYCARBONATE (@.1V)

Frequency	MEASURED Z(Ω)/Phase Angle (°)	CALCULATED Z(Ω)/Phase Angle (°)
	CYLINDRICAL SAMPLE	
10 kHz	66.080/-0.011	155.350/-0.63
100 kHz	66.047/-0.081	158.50 /-1.3
1 MHz	65.933/-0.548	154.330/-4.5
10 MHz	66.951/-3.845	157.550/-7.2
	RECTANGULAR SAMPLE	
10 kHz	127.50/-0.014	171.01 /-1.05
100 kHz	127.41/-0.198	192.53 /-3.85
1 MHz	126.90/-1.661	215.80 /-6.88
10 MHz	121.38/-11.574	235.80 /-15.56

TABLE 3. GRAPHITE FIBER COMPOSITE TEST COMPARISON

Samples of 40% graphite fibers and particles were also fabricated in polycarbonate and measured for shielding effectiveness in the ASTM dual chamber box. EMI Shielding for the PAN fibers ranged from 60dB at 15 MHz to 40dB at 1 GHz and from 53dB at 15 MHz to 36dB at 1 GHZ. Calculations based upon complex impedance and using the model developed gave values that were 10 to 22% below the measured values for the fiber and 12 to 28% below the measured value for the particles. These values are not vastly different from those found in the literature[13].

CONCLUSIONS

The results shown in Table 3 indicate that there is at least order-of-magnitude agreement with the initial model. However, fiber alignment is extremely important in the calculation and the exact place this alignment factor plays in the model is elusive. Further tests on non-aligned (particle) samples indicate that, at the time of this writing, particulate samples tend to be more predictable than are fiber samples. Though variances are noted in this model, initial results are encouraging in that it appears to be a parametric model that can predict basic electrical properties of composites, at least at lower frequencies. Other data is being assembled and refinements on the initial model are being made. The authors feel that this approach is indeed a viable one for design and will be pursued by testing and modifications as dictated by results and feedback.

ACKNOWLEDGMENTS

Support for this project was provided by the Office of The Chief of Naval Research/Office of Naval Technology; Submarine Techhnology Program Element; Program Element Manager is Mr. Gene Remmers, Code 233. Block Program Manager is Mr. Lincoln Cathers, Code 012.4, of the David Taylor Naval Ship Research & Development Center. Principal Investigator of "The Ships Below-Decks EMC Program" is Mr. David S. Dixon, of the Naval Underwater Systems Center, Code 3431.

REFERENCES

1. Nangrani, K.J., "The Effect of Additives and Molecular Weight on Flow and EMI Shielding Properties of Conductive Composites of Polycarbonates", Interference Technology Master, R&B Enterprises, 1986. p.165.

2. Private Communication. M. Avoux, G&H Technology. June, 1986.

3. Mott, N.F., Advanced Physics (Philos. Mag. Suppl.), 16:49 (1967).

4. McCullough, R.L., Composites Science and Technology, 22:3 (1985).

5. Bhattacharya, S.K., "Metal Filled Polymers: Properties and Applications", Marcel Dekker, N.Y., 1986. pp. 170, ff.

6. Sichel, E.K., "Carbon Black-Polymer Composites", Marcel Dekker, N.Y., 1982. pp. 152, ff.

7. Miyazaki, Y., Tominaga, S., and Tanka, M., "Electromagnetic Shield Properties of Plastics and Ceramics with Resistance and Conductance Particles", Tech. Report of IECE. Japan EMC J81-80 (1980).

8. Showalter, R.E. and Snyder, C.H., IEEE Trans. on Circuits and Systems, CAS-33:7, 707-710 (1986).

9. Pike, J.N., Private Communication, UCRI 618 (1970).

10. op. cit. ref. 7, p. 155.

11. Stan, L., Ceramic Bulletin, 65:9, 1293-1296 (1986).

12. Sichel, E.K., et al., J. Electron. Mater. 22:3, 77 (1982).

13. Reilly, J.J., Thoman, S.J., and LIN, W.W., SAMPE Journal, January/February, 1987. pp. 22-27.

INITIAL DISTRIBUTION LIST

Addressee	No. of Copies
External	
NAVSEA (CHENG-T (W. White); PMS-350; SEA-06D, -06D4, -06D443, -06D444, -06DC (H. DeMattia), -06DE, -56Z1, -56Z2, -61R4)	11
NAVAIR (AIR-5161F)	1
CNO (OP-941FC (Dr. R. Haislmaier))	1
SPAWAR (32DT)	1
OCNR/ONT (Code 233 (G. Remmers), Code 234 (J. Cauffman))	2
DTNSRDC (Code 012.4 (L. Cathers))	1
UPenn (Contract N66604-87-R-1155 (Dr. R. Showers))	1
Western New England College (Contract N66604-87-E-434 (Dr. J. Masi))	1
G & H Tech., Inc., Camarillo Office (Contract N66604-87-C-1568)	1
DTIC	2